

**Università degli Studi di Napoli Federico II**  
**SCUOLA POLITECNICA E DELLE SCIENZE DI BASE**

---

**DIPARTIMENTO DI INGEGNERIA INDUSTRIALE**  
**Corso di Laurea in Ingegneria Aerospaziale**

**Tesi di Laurea in Ingegneria Aerospaziale**

# **Longitudinal stability of a commercial aircraft with a Mathcad-Based Software**

**Relatore:**

**Prof. A. De Marco**

**Candidato:**

**Giuseppe Alferi**

**Matricola N35/611**

---

**Anno Accademico 2013/2014**



---

# CONTENTS

---

<b>1</b>	<b>A Mathcad-based calculation framework for fast aircraft aerodynamic analysis</b>	<b>5</b>
1.1	Introduction . . . . .	5
1.2	Generalities on Semi-empirical models in aircraft aerodynamics . . . . .	5
1.2.1	Aircraft preliminary design and design automation . . . . .	6
1.2.2	Fast aircraft design . . . . .	7
1.3	Aerodynamic model of the complete aircraft . . . . .	8
1.3.1	Mathcad Prime 3.0 . . . . .	9
1.4	The aerodynamic database . . . . .	14
1.4.1	The HDF database format . . . . .	14
1.4.2	The HDFView tool . . . . .	16
1.4.3	Storage specifications . . . . .	17
1.4.4	Mathcad user-defined HDF access functions . . . . .	20
<b>2</b>	<b>Review of basic concepts of aerodynamic modeling</b>	<b>25</b>
2.1	Wing Related Parameters . . . . .	25
2.1.1	Geometrical Data . . . . .	25
2.1.2	Aerodynamic Parameters . . . . .	27
2.1.3	Downwash . . . . .	28
2.2	Horizontal Tail Related Parameters . . . . .	29
2.3	Longitudinal Stability . . . . .	30
2.3.1	General Parameters . . . . .	30
2.3.2	Fuselage Contribution evaluated using Multhopp's Method . . . . .	30
2.3.3	Aerodynamic Centre . . . . .	32
2.3.4	Lift Coefficients . . . . .	33
2.3.5	Coefficients at Stick-Fixed Conditions . . . . .	36
2.3.6	Stick-Free Conditions . . . . .	37
2.3.7	Total Lift and Drag Coefficients . . . . .	38
<b>3</b>	<b>Numerical test sample on Boeing 787 Dreamliner</b>	<b>39</b>
3.1	Boeing 787 Dreamliner . . . . .	40
3.2	Parameters research . . . . .	44
3.3	Main geometric parameters . . . . .	45

3.3.1	Wing related parameters . . . . .	45
3.3.2	Horizontal Tail related parameters . . . . .	45
3.3.3	Vertical tail related parameters . . . . .	46
3.3.4	Geometric fuselage parameters . . . . .	46
3.3.5	Operating points . . . . .	46
3.4	Longitudinal stability . . . . .	47
3.4.1	Lift coefficient dependent on $\alpha$ . . . . .	47
3.4.2	Determination of aerodynamic center for wing+fuselage . . . . .	48
3.4.3	Pitching coefficient dependent on $\alpha$ . . . . .	48
3.4.4	Lift coefficient dependent on $i_h$ . . . . .	48
3.4.5	Pitching coefficient dependent on $i_H$ . . . . .	49
3.4.6	Elevator's moment . . . . .	49
3.4.7	Stability analysis . . . . .	49
	<b>Bibliografia</b>	<b>51</b>



---

## A MATHCAD-BASED CALCULATION FRAMEWORK FOR FAST AIRCRAFT AERODYNAMIC ANALYSIS

---

### 1.1 Introduction

The goal of this thesis project has been improving a software tool for the preliminary analysis of aircraft stability and control at subsonic speeds. It has been set up to compute aerodynamic coefficients for longitudinal equilibrium. The calculation formulas are mostly based on the book by Napolitano [1] and USAF DATCOM [2]. The software is MARYSA, which stands for Mathcad Aircraft Preliminary Stability Analysis. This software is developed in Mathcad Prime 3.0, a high-level programming environment with a powerful interface for equations handling. This makes the software extremely user-friendly and helps analysing aircraft performances in several flight conditions and in different geometrical configurations. The change from the previous project is the use of a database created in a hierarchical data format (HDF), a file format designed to store and organized large amounts of numerical data, that contains all aerodynamic data both for longitudinal and lateral-directional equilibrium. In this chapter we introduce the structure of database and give some details about the MARYSA's algorithms developed.

### 1.2 Generalities on Semi-empirical models in aircraft aerodynamics

Aircraft stability and control is a subject of central importance in flight mechanics education. Specifically, in flight dynamics, controls, and aircraft design. Static and dynamic stability characteristics are evaluated by introducing an airplane aerodynamic model, that is, a formulation that permits the calculation of the resultant aerodynamic force and moment acting on the vehicle in given flight conditions. One of the most challenging aspects of introductory level flight mechanics learning is the effective and satisfactory explanation

of how the airplane's aerodynamic behaviour depends on the external shape and on flight conditions. Well-known semi-empirical formulations exist, mostly taken from the United States Air Force DATCOM (Data Compendium) [2] or the English ESDU (Engineering Sciences Data Unit, [www.esdu.com](http://www.esdu.com)), that allow designers to estimate the complete aircraft aerodynamic coefficients and stability derivatives. Most of these formulas involve the evaluation of quantities that are available as tabular (plotted) functions or as the output of nomograms. Engineers in the initial stages of aircraft design process do not know all the details of the external shape or the specifics of internal structures and are allowed to explore the effectiveness of their design by varying some of the geometric or physical parameters involved. This Thesis introduces an up-to-date learning approach designed to lower entry-level difficulties in aircraft stability and control studies. A fast aerodynamic analysis framework based on intuitive mathematical worksheets has been created in order to facilitate the learning process. The automated calculation tool give learners the opportunity to experiment with aircraft shape variations and to verify that the underlying models correctly represent the known physics phenomena. In the following sections the prominent aspects of aircraft stability and control education and the related challenges are discussed. Because of the important role that this subject matter plays in the broader subject of aircraft design, a background on this topic is also given. Successively a selection of typical semi-empirical formulas is reported in order to illustrate the difficulties found by younger learners in the analysis of airplane aerodynamics. Finally a set of mathematical worksheets specifically designed for fast semi-empirical evaluation of aerodynamic coefficients of a complete aircraft is introduced and discussed.

### 1.2.1 Aircraft preliminary design and design automation

Before going further, some specific topics related to the discipline of aircraft design have to be brought up and presented briefly. New aircraft are designed for a variety of reasons, but most are designed to fulfill a specific role or a mission as dictated by prospective customers. No matter the type of aircraft or the reason for its design, specific tasks must be completed before it can be built and flown. The order of these tasks is called the *design process*. The order of the tasks that constitute the design process may vary depending on the company involved. Generally, the actual process will depend on the size and maturity of the company in which it takes place and the order of tasks often varies. However, there are certain steps that must be completed in all of them; for instance, the estimation of weight; sizing of lifting surfaces and the fuselage; estimation of performance; and other essential tasks. Performance requirements must be clearly defined and are usually a part of the airplane's mission definition. It is imperative to quantify characteristics such as the takeoff distance, time to cruise altitude, cruise range, and even environmental noise for some types of aircraft. But it is also important to understand how deviations from the design conditions affect the performance (performance sensitivity). Moreover, aircraft handling issues related to stability and control aspects must be anticipated and their severity resolved. In general, the aircraft design process involves several distinct phases. These are referred to as: (i) Requirements phase, (ii) Conceptual design phase, (iii) Preliminary design phase, (iv) Detail design phase, and (v) Proof-of-concept aircraft construction and

testing phase.

The aircraft preliminary design phase is of special importance and ultimately answers whether the initial idea of the aircraft established in prior phases is viable. It not only exposes potential problems, as well as possible solutions to those problems, but yields a polished loft that will allow a flying prototype to be built. Some of the specific tasks that are accomplished during this phase are:

- Detailed aircraft geometry development,
- Layout of major load paths,
- Weight estimation,
- Details of mission,
- Performance,
- *Stability and control*,
- Evaluation of special aerodynamic features,
- Evaluation of certifiability,
- Evaluation of mission capability,
- Refinement of producibility,
- Assessment of maintainability issues,
- Preliminary production cost estimation.

In the early years of aircraft design, designers generally used analytical theory to perform the various engineering calculations relative to the preliminary design phase along with experimental testing. These calculations involved much work and were time consuming. The first attempts to automate the calculation process and to develop simplified relations and semi-empirical formulas date back to the 1940s. Even after simplifications, the calculations were still extensive and time consuming. With the introduction of computers, a majority of these calculations were automated; however, the lack of design visualization and the huge amount of required experimental testing kept the aircraft design a labour-intensive process. With the increasing development of programming languages, engineers were able to write programs and to develop codes that were tailored to design an aircraft. Originally, this was done using mainframe computers and with programming tools that lacked many of the features of modern integrated development environments (IDE) available today. With the introduction of personal computers, design programs started to feature a more user-friendly approach. With software and computer hardware currently available in aerospace industry the design process has become very effective and employs a very sophisticated, highly optimized chain of calculation tools.

### 1.2.2 Fast aircraft design

The study of flight mechanics of fixed-wing aircraft, is typically articulated in two clearly distinguishable parts. The first focuses on aircraft performance evaluation while the second deals with aircraft stability and control. The basic theory of airplane performance characteristics considers the vehicle as a point mass to which all the forces (lift, thrust, weight and drag) are applied. Though this requires a number of simplifying assumptions, this approach still provides learners with core knowledge of aircraft aerodynamics and performance. This will serve as a basis for further detailed studies. A prerequisite to

this subject is a basic knowledge of aerodynamics (e. g. polar curves and airfoil theory). Elements of propulsion systems are also necessary in a more or less concise way, at least to introduce propeller or jet-engine effects on the airplane behaviour. The above approach serves to introduce the equilibrium equations of an airplane in atmospheric flight. Standard reference frames are introduced in order to address the subjects of equilibrium or *trimmed* flight (translational and rotational). The second part deals with aircraft stability and control. In aircraft stability and control studies most of the aerodynamic effects on the whole aircraft are taken into consideration. For instance, the finite wing is modelled according to the classical lifting-line theory; the same is done for the downwash on the tail; the aerodynamic effects of the fuselage are studied with a certain detail. Moreover, a basic introduction to the unsteady aerodynamics phenomena and the effects of airplane angular speeds are necessary. The overall aircraft model is then further improved by considering engineering correction coefficients accounting for interaction effects between various elements of the aerodynamic configuration. At a basic level the main aerodynamic effects are linearized; thus the subject is simplified by the validity of the superposition principle. Nevertheless, despite this conceptual simplicity, when discussing how aerodynamic coefficients depend on aircraft geometric parameters (wing aspect ratio, wing sweep, fuselage fineness ratio, tail volumetric parameters, etc.) and on flight conditions (altitude, flight Mach number, etc.) many semi-empirical formulas come into play. These formulas are taken mostly from the USAF DATCOM or the English ESDU (Engineering Sciences Data Unit, [www.esdu.com](http://www.esdu.com)) and many of them involve the evaluation of coefficients that are available as tabular/plotted functions. The collection of all these elements provides a fairly articulated picture of the topics treated in flight mechanics.

The correct estimation of some physically complex contributions to aircraft aerodynamic coefficients requires the evaluation of ‘semi-empirical’ (or ‘semi-analytical’) formulas, which often refer to technical graphs. These are nothing but functions of one, two or more variables (lookup tables put in graphical forms) that were obtained from experimental investigations or more complex theoretical models. Practical application of the various formulas, sometimes resulting from a cascade of complex concepts, is typically recognized as the best method to fully understand the aircraft aerodynamic modeling.

### 1.3 Aerodynamic model of the complete aircraft

The details of the aerodynamic model considered in this work are found in the textbook by Napolitano [1], to which the reader is referred to. The model is based on a set of formulas expressing the aerodynamic coefficients  $C_D$ ,  $C_L$ ,  $C_M$ ,  $C_Y$ ,  $C_X$  and  $C_N$  at given flight conditions, for the specified airplane’s geometry. These well-known formulas, mostly based on the USAF DATCOM [2], take into account the contributions of wing, fuselage and tail planes and are of semi-empirical nature. Each contribution, in most of the cases, is estimated by entering one or more graphs.

$$\begin{aligned}
A_{c_{W_1}} &:= \frac{2 \cdot (c_{W_{t_1}} - c_{W_{r_1}})}{b_{W_1}} = -0.657 & B_{c_{W_1}} &:= c_{W_{r_1}} = 15.57 \text{ m} & f_{c_1}(y) &:= A_{c_{W_1}} \cdot y + B_{c_{W_1}} \\
A_{c_{W_2}} &:= \frac{2 \cdot (c_{W_{t_2}} - c_{W_{r_2}})}{b_{W_2}} = -0.323 & B_{c_{W_2}} &:= c_{W_{r_2}} = 8.51 \text{ m} & f_{c_2}(y) &:= A_{c_{W_2}} \cdot \left( y - \frac{b_{W_1}}{2} \right) + B_{c_{W_2}} \\
A_{\varepsilon_{W_1}} &:= \frac{2 \cdot \varepsilon_{W_1}}{b_{W_1}} & B_{\varepsilon_{W_1}} &:= 0 \text{ deg} & f_{\varepsilon_{g_1}}(y) &:= A_{\varepsilon_{W_1}} \cdot y + B_{\varepsilon_{W_1}} \\
A_{\varepsilon_{W_2}} &:= \frac{2 \cdot (\varepsilon_{W_2} - \varepsilon_{W_1})}{b_{W_2}} & B_{\varepsilon_{W_2}} &:= \varepsilon_{W_1} & f_{\varepsilon_{g_2}}(y) &:= A_{\varepsilon_{W_2}} \cdot \left( y - \frac{b_{W_1}}{2} \right) + B_{\varepsilon_{W_2}}
\end{aligned}$$

**Figure 1.1** Chord and geometric twist angle spanwise distribution .

### 1.3.1 Mathcad Prime 3.0

Mathcad [www.ptc.com/product/mathcad](http://www.ptc.com/product/mathcad) is a powerful mathematical spreadsheet application for the Microsoft Windows operating system. Mathcad allows the user to easily handle complicated mathematical operators such as finite integrals and derivatives, loop calculations, limits and numerical series. Moreover, the format of a generic mathematical function has a clear layout, like one written on a paper work and this helps to sort out any kind of equation however complex. This work is based on the specific product named Mathcad Prime 3.0, also available in the Express edition. Mathcad Prime 3.0 Express [www.ptc.com/product/mathcad/free-trial](http://www.ptc.com/product/mathcad/free-trial) is a free, limited-functionality version which is able to read and execute projects created with the fully functional version of the software. Beside the mathematical tools, Mathcad has a high-level programming language which is easy to be learned and applied since it shows a command window where all basic functions can be found (i.e. if, for, while and so forth). Mathcad manages work sheet from top to down and from left to right and it lets to include a work sheet in another, in a sort of 'Matryoshka structure', so calculating the most external one, Mathcad calculates all those included in external one. Mathcad reads also custom functions wrote by users to perform certain tasks that base program doesn't perform. Last but not least, Mathcad reads, saves and processes data sets taken from files in Comma-Separated Values format (CSV, extension .csv) or native Microsoft Excel format (extension .xlsx).

The aircraft model has been implemented as a set of Mathcad worksheets and the access to the tabular functions is based on custom-made Mathcad functions (packaged into a specific DLL). Fragments of worksheets showing the typical live mathematical implementation provided by Mathcad are shown in the following figures: 1.1, 1.2, 1.3, 1.4, 1.5, 1.6, 1.7, 1.8, 1.9.

$$\alpha_{0L\_W\_1} := \frac{2}{S_W} \cdot \int_0^{\frac{b_{W\_1}}{2}} f_{-c_1}(y) \cdot (f_{-\alpha_{0L\_2D\_1}}(y) - f_{-\varepsilon_{g\_1}}(y)) dy = -0.019 \quad \alpha_{0L\_W\_1} = -1.1 \text{ deg} \quad \bullet \text{ Alpha Zero Lift 3D Inner Panel}$$

$$\alpha_{0L\_W\_2} := \frac{2}{S_W} \cdot \int_{\frac{b_{W\_1}}{2}}^{\frac{b_W}{2}} f_{-c_2}(y) \cdot (f_{-\alpha_{0L\_2D\_2}}(y) - f_{-\varepsilon_{g\_2}}(y)) dy = -0.004 \quad \alpha_{0L\_W\_2} = -0.23 \text{ deg} \quad \bullet \text{ Alpha Zero Lift 3D Outer Panel}$$

$$\alpha_{0L\_W} := \frac{2}{S_W} \cdot \int_0^{\frac{b_W}{2}} c(y) \cdot (\alpha_{0L\_2D}(y) - \varepsilon_g(y)) dy = -0.023 \quad \alpha_{0L\_W} = -1.33 \text{ deg} \quad \bullet \text{ Alpha Zero Lift 3D}$$

Figure 1.2 Wing zero lift angle calculation.

• Polhamus formula

$$f_{-k_1}(M, M_{cr\_3D}, A_{LE}, \lambda, AR) := \begin{cases} \text{if } (M < M_{cr\_3D}) \wedge (A_{LE} < 32 \text{ deg}) \wedge (\lambda > 0.4) \wedge (\lambda < 1) \wedge (AR > 3) \wedge (AR < 8) \\ \quad \text{if } AR < 4 \\ \quad \quad \text{out} \leftarrow 1 + \frac{AR \cdot (1.87 - 0.000233 \cdot A_{LE})}{100} \\ \quad \text{else} \\ \quad \quad \text{out} \leftarrow 1 + \frac{((8.2 - 2.3 \cdot A_{LE}) - AR \cdot (0.22 - 0.153 \cdot A_{LE}))}{100} \\ \quad \text{else} \\ \quad \quad \text{out} \leftarrow 100 \\ \quad \text{return out} \end{cases}$$

Valid only if:

- $M < M_{crit}$   $M_\infty = 0.65$   $M_{cr\_W\_3D} = 0.803$
- $A_{LE} < |32^\circ|$   $A_{W\_LE\_eqv} = 34.5 \text{ deg}$
- $3 < AR < 8$   $AR_{W\_eqv} = 7.916$
- $0.4 < \lambda < 1$   $\lambda_{W\_eqv} = 0.162$

$$k_{Polhamus} := f_{-k_1}(M_\infty, M_{cr\_W\_3D}, A_{W\_LE\_eqv}, \lambda_{W\_eqv}, AR_{W\_eqv}) = 100$$

• Airfoil lift-curve slope at MAC

$$C_{l\alpha@MAC\_W} := C_{l\alpha\_W}(Y_{MAC\_W\_crk}) = 6.972$$

$$f_{-C_{l\alpha\_W}}(M, k_P, AR, A_{c2}, C_{l\alpha@MAC}, A_{LE}) := \begin{cases} \text{if } k_{Polhamus} \neq 100 \\ \quad \text{out} \leftarrow \frac{2 \cdot \pi \cdot AR}{2 + \sqrt{\left( \frac{AR^2 \cdot (1 - M^2)}{k_P^2} \left( 1 + \frac{\tan(A_{c2})^2}{(1 - M^2)} \right) \right) + 4}} \\ \quad \text{return out} \\ \text{else} \\ \quad a_0 \leftarrow \frac{C_{l\alpha@MAC\_W}}{\sqrt{1 - M^2} \cdot \cos(A_{LE})} \\ \quad \text{out} \leftarrow \frac{a_0 \cdot \cos(A_{LE})}{\sqrt{1 - (M \cdot \cos(A_{LE}))^2 + \left( \frac{a_0 \cdot \cos(A_{LE})}{\pi \cdot AR} \right)^2}} + \frac{a_0 \cdot \cos(A_{LE})}{\pi \cdot AR} \\ \quad \text{return out} \end{cases}$$

Polhamus Formula

Alternative Formula

Figure 1.3 Lift slope coefficient calculation.



Figure 1.4 Cranked wing with aerodynamic mean chords visualization.

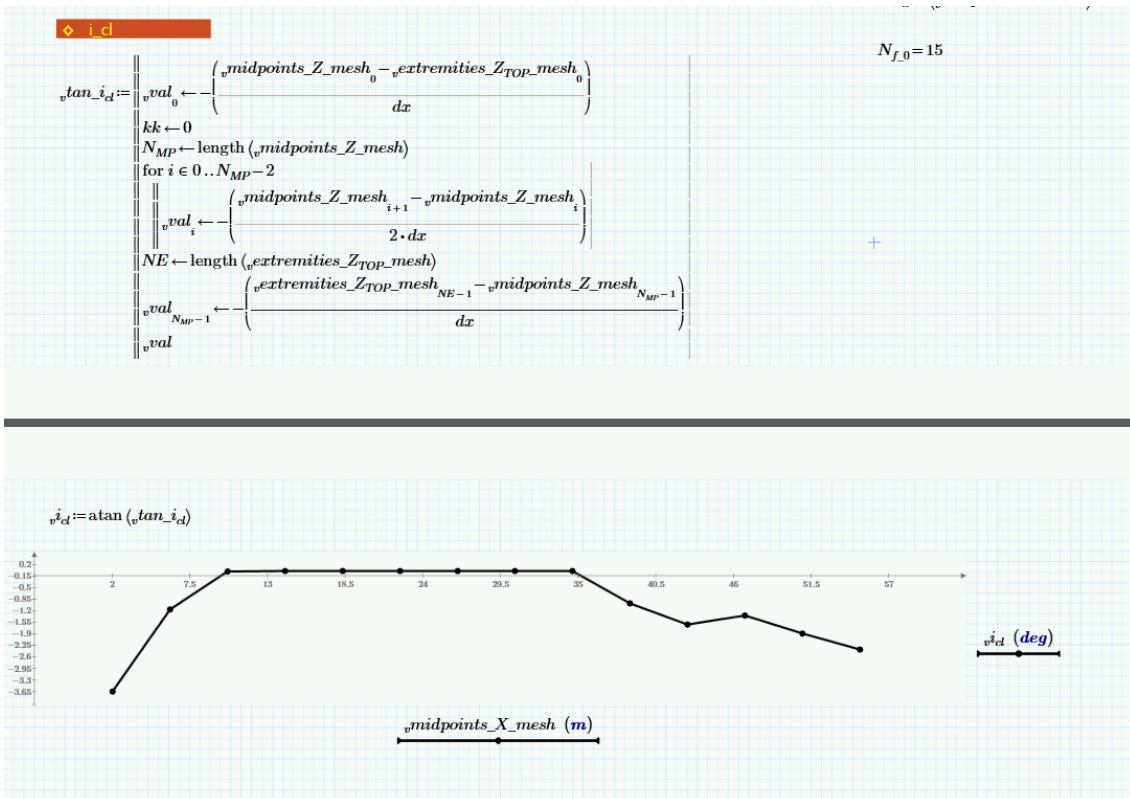


Figure 1.5 Local tangent slope at fuselage camber line.



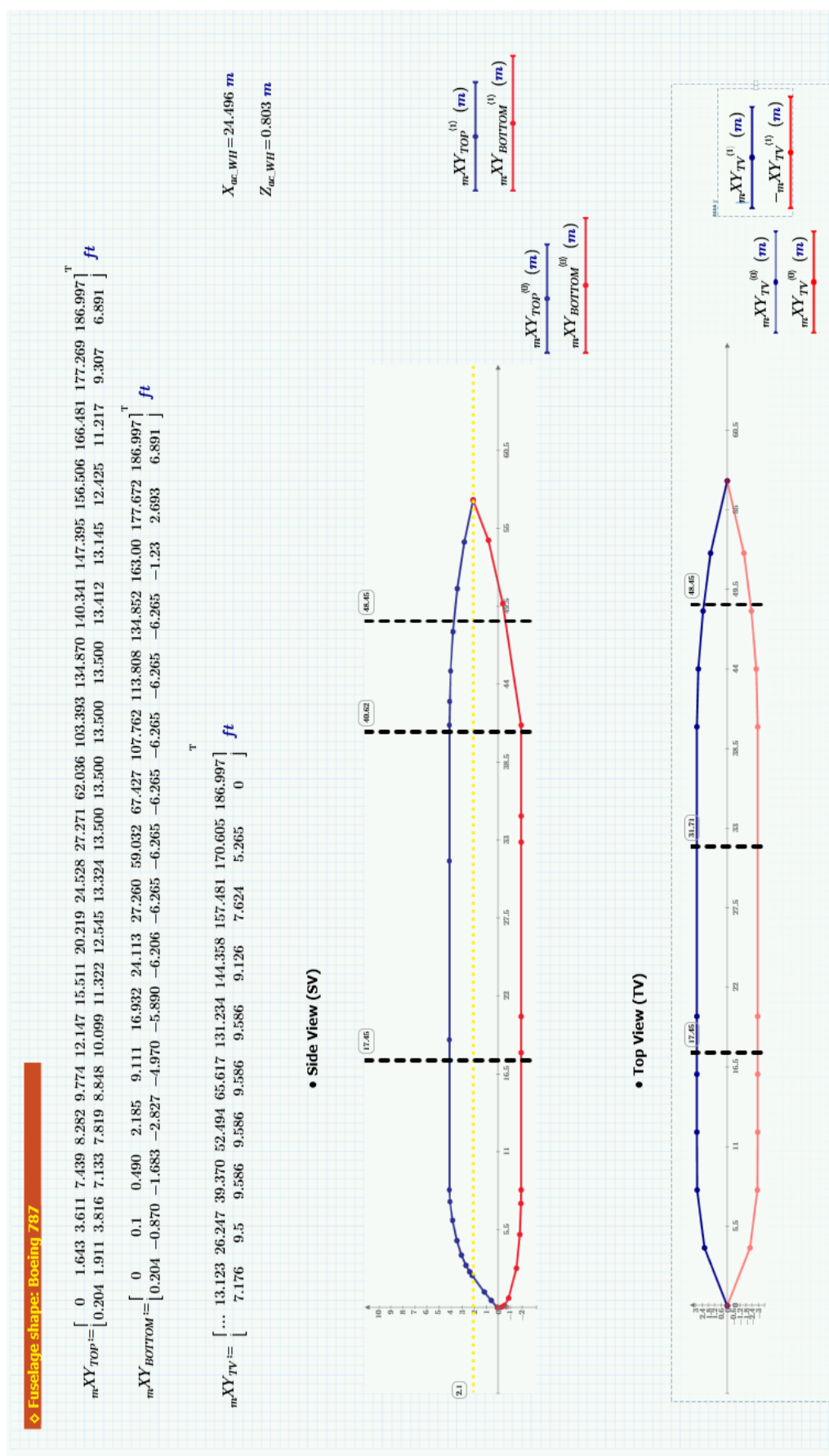


Figure 1.6 Fuselage shape.



$$C_{L\delta e} := C_{L\alpha_H} \cdot \eta_H \cdot \frac{S_H}{S_W} \cdot \tau_e = 0.415$$

#### Wing-Body-HTail Momentum Coefficient Curve Slope

$$C_{M0_f} = -0.048 \quad C_{Mac_W} = -0.017 \quad \xi_{CG} - \xi_{ac_{WB}} = -0.238 \quad \varepsilon_0 = 0.034$$

$$C_{M0_{WB}} := C_{Mac_W} + C_{M0_f} = -0.065$$

$$C_{M0} := C_{M0_{WB}} + C_{L0_{WB}} \cdot (\xi_{CG} - \xi_{ac_{WB}}) + \eta_H \cdot C_{L\alpha_H} \cdot VolumeRatio_H \cdot \varepsilon_0 + C_{Mac_H} = -0.078$$

$$C_{M\alpha} := C_{L\alpha_{WB}} \cdot (\xi_{CG} - \xi_{ac_{WB}}) - \eta_H \cdot C_{L\alpha_H} \cdot VolumeRatio_H \cdot (1 - d\varepsilon_{d\alpha_H}) = -3.187$$

$$C_{MiH} := -(\eta_H \cdot C_{L\alpha_H} \cdot VolumeRatio_H) = -2.975$$

$$C_{M\delta e} := -(\eta_H \cdot C_{L\alpha_H} \cdot VolumeRatio_H) \cdot \tau_e = -1.339$$

#### Unsteady flight coefficients

$$\alpha_{dot} = 21.486 \frac{deg}{s} \quad q = 2.55 \frac{deg}{s} \quad u = 20 \frac{m}{s}$$

$$\alpha_{dot_{bar}} = 0.006 \quad q_{bar} = 7.542 \cdot 10^{-4} \quad u_{bar} = 0.079$$

Figure 1.7 Momentum coefficient calculation.

$$C_{D\alpha} := \frac{2 \cdot C_L \cdot C_{L\alpha}}{\pi \cdot AR_W \cdot e_{TOT}} = 0.275 \text{ rad}^{-1}$$

#### Neutral Point

$$\xi_N := \frac{\xi_{ac_{WB}} + \frac{C_{L\alpha_H}}{C_{L\alpha_{WB}}} \cdot \eta_H \cdot \frac{S_H}{S_W} \cdot (1 - d\varepsilon_{d\alpha_H}) \cdot \xi_{AC_H}}{1 + \frac{C_{L\alpha_H}}{C_{L\alpha_{WB}}} \cdot \eta_H \cdot \frac{S_H}{S_W} \cdot (1 - d\varepsilon_{d\alpha_H})} = 0.65 \quad \bullet \text{ Neutral Point}$$

$$SSM := \xi_{CG} - \xi_N = -0.4$$

• Static Stability Margin --> Check

$$\frac{C_{M\alpha}}{C_{L\alpha}} = -0.4$$

#### Stability Coefficients at Stick-Free Condition

$$F := 1 - \tau_e \frac{C_{h_{\alpha e}}}{C_{h_{\delta e}}} = 0.774$$

$$C_{M0_{free}} := C_{M0_{WB}} + C_{L0_{WB}} \cdot (\xi_{CG} - \xi_{ac_{WB}}) + \eta_H \cdot C_{L\alpha_H} \cdot VolumeRatio_H \cdot \varepsilon_0 \cdot F + C_{Mac_H} = -0.101$$

Figure 1.8 Neutral point calculation.

**I<sub>H</sub> variation**

$$i_H := [0 \quad -1 \quad -2 \quad -3] \text{ deg} \quad i_{H,1} := i_{H0,0} = 0 \quad i_{H,2} := i_{H0,1} = -1 \text{ deg} \quad i_{H,3} := i_{H0,2} = -2 \text{ deg}$$

```

Equilibrium_i_H(a) :=
|| angle_position_in_i_H ← a
|| i ← 0
|| for i ∈ 0, 1..a-1
||   zero_lift_coeff_htail ← C_Lα_H · (i_H0,i - α0L_H) · (1 - dε_dα_H)
||   zero_lift_coeff ← C_L0_WB - C_Lα_H · VolumeRatio_H · ε_0 + zero_lift_coeff_htail
||   array_constants ← [ C_L - zero_lift_coeff - C_LiH · i_H0,i ]
||                     [ C_M - C_M0 - C_MiH · i_H0,i ]
||   solution ← lsolve(M, array_constants)

```

$$Equilibrium_{i_H}(1) = \begin{bmatrix} -0.182 \\ -2.91 \end{bmatrix} \text{ deg} \quad Equilibrium_{i_H}(2) = \begin{bmatrix} 0.146 \\ -1.469 \end{bmatrix} \text{ deg} \quad Equilibrium_{i_H}(3) = \begin{bmatrix} 0.474 \\ -0.028 \end{bmatrix} \text{ deg} \quad Equilibrium_{i_H}(4) = \begin{bmatrix} 0.803 \\ 1.413 \end{bmatrix} \text{ deg}$$

Figure 1.9 Horizontal tail  $i_H$  variation.

## 1.4 The aerodynamic database

The semi-empirical aerodynamic formulation upon which the proposed calculation tool is based accesses directly to a unique file that stores all the information needed by the several implemented formulas. The database file is binary file formatted according to the Hierarchical Data Format (HDF, [www.hdfgroup.org](http://www.hdfgroup.org)).

### 1.4.1 The HDF database format

Hierarchical Data Format (HDF, HDF4, or HDF5) is the name of a set of file formats and libraries designed to store, manage, preserve and extract maximum use of scientific data in the face of enormous growth in size and complexity, enhancing the reliability of archived data and promoting the use of standardized data formats. This is a kind of data whose value to society will continue over decades and in some cases over centuries. An example of such data is the Earth Observing System (EOS), which already contains three petabytes (3 million billion bytes) of data, and will by project-end contain 15 petabytes. EOS is just one of a growing number of projects that face the same dilemmas and have similar potential. There are other remote-sensing projects, such as the National Polar Orbiting Environmental Satellite System, which will dwarf EOS. HDF technologies are relevant when the data challenges being faced push the limits of what can be addressed by traditional database systems, XML (eXtensible Markup Language) documents, or in-house data formats. Leveraging the powerful HDF products and the expertise of The HDF Group, organizations realize substantial cost savings while solving challenges that seemed intractable using other data management technologies. Many HDF adopters have very large datasets, very fast access requirements, or very complex datasets. Others turn to HDF because it allows them to easily share data across a wide variety of computational platforms using applications written in different programming languages. Some use HDF to take advantage of the many open-source and commercial tools that understand HDF. Similar to XML documents, HDF files are self-describing and allow users to specify complex data relationships and dependencies. In contrast to XML documents, HDF files can contain binary data (in many representations) and allow direct access to parts of the file without first parsing the entire contents. HDF, not surprisingly, allows hierarchical data objects to be expressed in a very natural manner, in contrast to the tables of relational database. Whereas relational databases support tables, HDF supports  $n$ -dimensional datasets and each element in the dataset may itself be a complex object. Relational databases offer excellent support for queries based on field matching, but are not well-suited for sequentially processing all records in the database or for subsetting the data based on coordinate-style lookup. In-house data formats are often developed by individuals or teams to meet the specific needs of their project. While the initial time to develop and deploy such a solution may be quite low, the results are often not portable, not extensible, and not high-performance. In many cases, the time devoted to extending and maintaining the data management portion of the code takes an increasingly large percentage of the total development effort - in effect reducing the time available for the primary objectives of the project. HDF offers a flexible format and powerful API backed by over 20 years of development history. Projects can

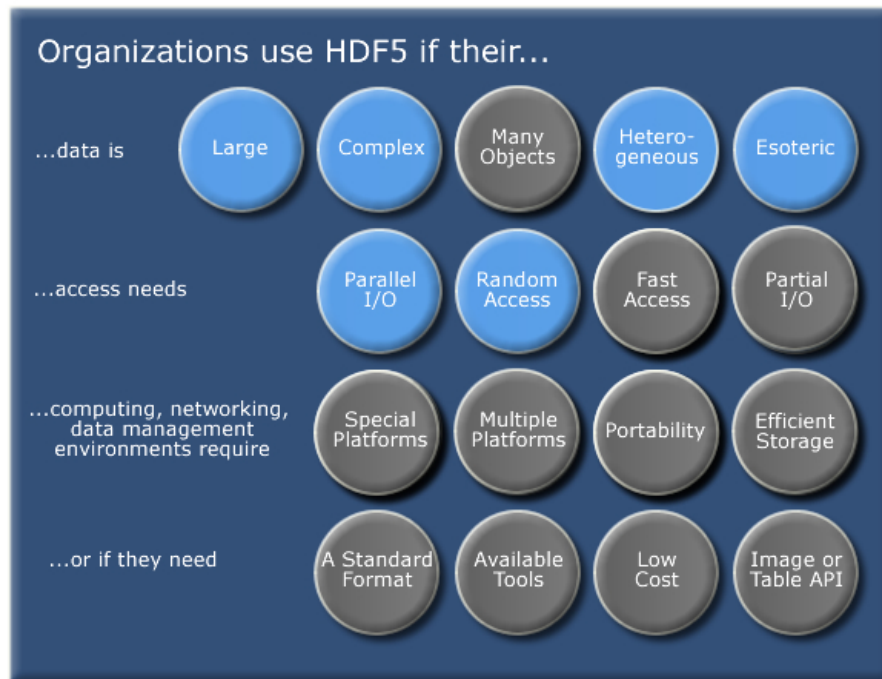


**Figure 1.10** Some of the data challenges facing HDF adopters.

leverage HDF's capabilities and still define their own data objects and project-specific API to those objects.

HDF5 supports an unlimited variety of datatypes, and is designed for flexible and efficient I/O and for high volume and complex data. The HDF5 technology suite includes:

- A versatile data model that can represent very complex data objects and a wide variety of metadata.
- A completely portable file format with no limit on the number or size of data objects in the collection.
- A software library that runs on a range of computational platforms, from laptops to massively parallel systems, and implements a high-level API with C, C++, Fortran 90, and Java interfaces.
- A rich set of integrated performance features that allow for access time and storage space optimizations.

In one experiment a  $53000 \times 53000$  image from a DNA sequencing analysis was stored in HDF5 and viewed. In another, using HDF5's external storage capability, a composite of 900 files from a seismic simulation was organized in HDF5 to create a terabyte-sized dataset, permitting fast subsetting. An aerospace company will archive all instrument data from a test flight, creating an HDF5 file of nearly a terabyte per test flight.

The HDF5 format and software include features specifically designed to store and access large datasets. There is no theoretical limit to the size of datasets that can be stored in an HDF5 file. HDF5 includes storage options, such as chunking, compression, and external object storage that mitigate many problems associated with large datasets. The flexible structure of HDF5 files makes it possible for applications to create composite structures, such as tables and indexes, that can provide fast random access to very large datasets. The HDF5 library includes sophisticated subsetting operations that offer very

fast access to portions of very large datasets. HDF5 supports certain kinds of parallel I/O, making it possible to read and write data at very high speeds.

The Earth Observing System's HDF-EOS format, based on HDF4 and HDF5, can store swaths, grids, in-situ data, instrument metadata, and browse images in a single file, making it possible to capture the entire collection of information about a day's mission. The grouping structure in HDF5 enables applications to organize data objects in HDF5 to reflect complex relationships among objects. The rich collection of HDF5 datatypes, including datatypes that can point to data in other objects, and including the ability for users to define their own types, lets applications build sophisticated structures that match well with complex data. The HDF5 library has a correspondingly rich set of operations that enables applications to access just those components that are important.

A government test center has more than 800,000 HDF5 files, each corresponding to a single test, where all of the information for the test is stored, including the measurements from every on-board instrument, GIS information about the location of the vehicle, browse image plots of the instrument data, and all metadata about the test run. Because one can mix and match any kind of data within an HDF5 file, applications are able to create coherent repositories of highly heterogeneous collections. One can mix tables, images, small metadata, streams of data from instruments, and structured grids all in the same file. New objects can be easily added to existing HDF5, even though the file was not originally created to handle the new objects.

HDF5 itself places no special meaning to data stored in datasets or attributes. An application can thus store any kind of data simply as a stream of bytes in a dataset or attribute. Using other features in HDF5, an application can provide metadata, indexes, and other information structures to provide full meaning to the data. Doing this in HDF5 then enables the applications to apply other features of HDF5, such as performance-enhancing features (fast I/O, compression), and access features (partial I/O).

The HDF5 format and library are designed to support parallel I/O.

When data is read from or written to a dataset in HDF5, an application can specify the subset of elements within the dataset's array that are to be read or written. The subset can be an n-dimensional rectangular section, it can be a set of points, or it can be a combination many rectangles and sets of points. A stride can be specified to take samples (e.g. every 10th row and column), and sequences of blocks can be accessed. The HDF5 'reference' datatype lets applications store information about regions of interest in a dataset, then apply this information in doing the partial I/O operations. Chunking helps optimize access to very large arrays, when partial access is desired. Only those chunks are accessed that contain the elements of interest. Even when datasets are compressed, only those chunks that contain the elements of interest need to be read or written and uncompressed. The grouping structure in HDF5 enables applications to organize data in ways that make it easy to find and access those components that are of interest, ignoring the others.

### 1.4.2 The HDFView tool

HDFView is a visual Java-based tool for browsing and editing HDF4 and HDF5 files (see Figure 1.15). HDFView allows users to browse through any HDF4 and HDF5 file, starting

with a tree view of all top-level objects in an HDF file's hierarchy. HDFView allows a user to descend through the hierarchy and navigate among the file's data objects. The content of a data object is loaded only when the object is selected, providing interactive and efficient access to HDF4 and HDF5 files. HDFView editing features allow a user to create, delete, and modify the value of HDF objects and attributes. The HDFView graphical user interface (GUI) is simple and easy-to-use. First, HDFView was implemented by using the Java 2 Platform, which is machine-independent. The GUI components have the same look-and-feel for all machines. Second, HDFView uses conventional folders and icons to display groups and datasets in a tree structure. Users can easily expand or collapse folders to navigate the hierarchical structure of an HDF file. Third, HDFView shows data content as text (table or plain text) or as image.

### 1.4.3 Storage specifications

HDFView was used to create an aerodynamic database. This database is made by a single file called

`Aerodynamic_Database_Ultimate.h5`

There are several groups within it, each one is associated to an aerodynamic coefficient. The group's name describes unequivocally the data that contains; it is composed by:

- a first string in brackets which explains to which aerodynamic term the group is referred to,
- a second string, which explains the axes labels,
- a third string, in brackets, which describes the parameter that defines each curve,
- a fourth string, in brackets, which describes the parameter that defines each group of curves,
- a final string, if necessary, which describes the further parameter that defines each group of curves.

The following is an example string used to name a group of data:

```
(C_l_delta_a)_RME_vs_ ...
...eta_(Lambda_beta)_(beta_times_AR_over_k)_(lambda)
```

Examples of plotted functions used for aerodynamic modelling are shown in Figure 1.11.

An exception may occur when you deal with nomograms. In this case, starting from the third string, each string in brackets refers, in order, to the parameter which describes each group of curves, as the following examples shows:

```
(C_n_beta_b)_K_N_times_1e-3_vs_x_cg_over_ ...
...l_b_(squared_l_b_over_S_b_s)_(square_root_(h1_over_h2))_ ...
...(h_b_over_w_b)
```

See, for example, Figure 1.12.

In each group there are:

- a *dataset* per each independent variable referred to the group dealing with. According to the origin of a matrix indexes used in HDF (first element is indexed as (0,0) and not as (1,1), i.e. zero-based indexing is assumed), let  $i$  be a natural number between 0 and  $n$ , with  $n$  counting the number of the independent variables ( $n = 0, 1, \dots, 3$ ). Then,

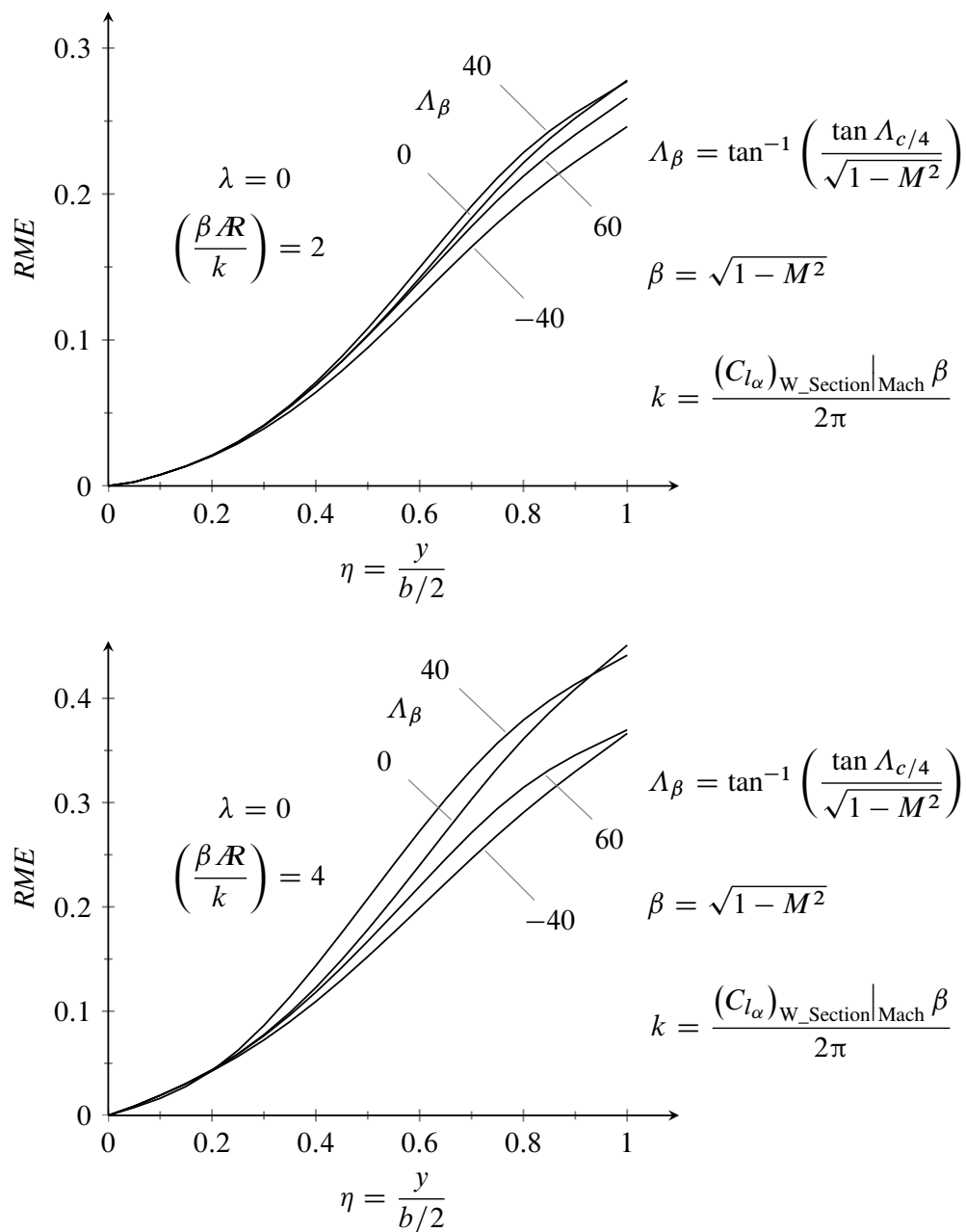


**Figure 1.11** Examples of plotted functions used for aerodynamic modelling.



$\text{var}_i$  is a vector containing the values of the  $i$ -th variable starting from the last one in the group's name till the innermost one;  $\text{var}_n$  will always contain values on  $x$ -axis. So, if:

- $n = 0$ : we have only one curve and  $\text{var}_0$  will be referred to  $x$ -axis values;
- $n = 1$ : we have more than one curve;  $\text{var}_0$  will be referred to the parameter which distinguishes each curve,  $\text{var}_1$  will be referred to  $x$ -axis values;
- $n = 2$ : we have more than one group of curves;  $\text{var}_0$  will be referred to the parameter which distinguishes each group of curves,  $\text{var}_1$  will be referred to the parameter which distinguishes each curve,  $\text{var}_2$  will be referred to  $x$ -axis values;
- $n = 3$ : we have two parameters which distinguish each group of curves;  $\text{var}_0$  will be referred to the first parameter which distinguishes each group of curves,  $\text{var}_1$  will be referred to the second parameter which distinguishes each group of curves,  $\text{var}_2$  will be referred to the parameter which distinguishes each curve,  $\text{var}_3$  will be referred to  $x$ -axis values;
- a dataset called `data`. It is a  $(n + 1)$ -dimensional array containing the output values. So, if:
  - $n = 0$ : we have a  $(a \times 1)$  two-dimensional array, that is a vector, where  $a$  is equal to  $\text{length}(\text{var}_n)$  containing  $y$ -axis values;
  - $n = 1$ : we have a  $(a \times b)$  two-dimensional array, where  $b$  is equal to  $\text{length}(\text{var}_{n-1})$ . Let  $j$  be a natural number between 0 and  $b$ ; then the  $j$ -th column will contain the output values referred to the  $j$ -th value of  $\text{var}_0$ ;
  - $n = 2$ : we have a  $(a \times b \times c)$  three-dimensional array, where  $c$  is equal to  $\text{length}(\text{var}_{n-2})$ . Let  $k$  be a natural number between 0 and  $c$ ; then the  $(j, k)$ -th column will contain the output values referred to the  $j$ -th value of  $\text{var}_1$  and the  $k$ -th value of  $\text{var}_0$ ;
  - $n = 3$ : we have a  $(a \times b \times c \times d)$  four-dimensional array, where  $d$  is equal to  $\text{length}(\text{var}_{n-3})$ . Let  $z$  be a natural number between 0 and  $d$ ; then the  $(j, k, z)$ -th column will contain the output values referred to the  $j$ -th value of  $\text{var}_2$ , the  $k$ -th value of  $\text{var}_1$  and the  $z$ -th value of  $\text{var}_0$ . In this case, there is also a `data_z` per each value of  $\text{var}_0$ , so that fixed  $z$ , we are in the same situation as the former point.
- an image per each group of curves. So, if:
  - $n = 0, 1$ : we have only one image called `plots`;
  - $n = 2$ : we have a number of images equal to the value of  $\text{length}(\text{var}_0)$ , called `plots_0`, `plot_1`, etc.;
  - $n = 3$ : we have a number of images equal to the value of  $\text{length}(\text{var}_0)$  times  $\text{length}(\text{var}_1)$ , called `plots_0_0`, `plots_0_1`, `plots_0_2`, etc.

Exceptions occur when you deal with monograms. Let  $i$  and  $j$  be natural numbers, belonging to  $[0, +\infty]$  and  $[0, 1]$ , respectively. In this case we will have:

- $\text{var}_{i_j}$ , which is a vector containing the values of the  $j$ -th independent variable referred to the  $i$ -th diagram.
- `data_i`, which is a bidimensional array containing the output values concerning the  $i$ -th diagram. Its structure is the same as  $(a \times b)$  arrays described above.
- an image called `plots` where all the group of curves are shown.

Each dataset is associated to a schedule, which can be seen in Show Properties menu

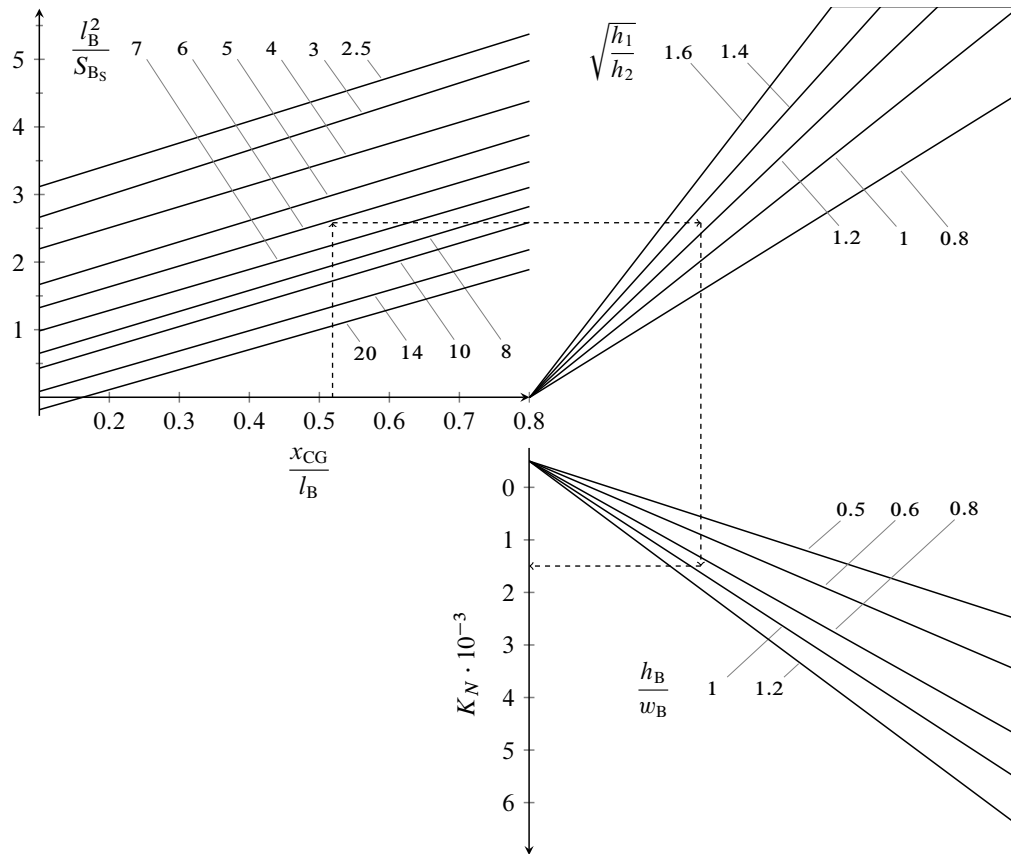


Figure 1.12 An example of nomogram.

of HDFView, containing three its mean *Attributes*:

- **description**: is a 1024-characters max length string, which describes the dataset;
- **n\_vars**: is a 256-characters max length string, that shows the independent variables from which the dataset values are depending of. It is assumed equal to 1, for independent variables themselves.
- **units**: is a 256-characters max length string, that shows the unit of the dataset variable. It is always written in capital letters.

Each group also contains a **note** field, that is a more accurate description about the group itself, the aerodynamic coefficients dealing with and the variables involved. Some groups also contain an **image** called **image** that shows some particular geometrical quantity used in the group itself.

#### 1.4.4 Mathcad user-defined HDF access functions

Mathcad does not have own built-in functions to read HDF files. As a consequence, a set of user-defined functions have been created and packaged into a unique DLL (Dynamic-link library). Three main functions have been written:

- **f\_HDF5Read\_FGD**, used to read a dataset within a specified group, within the HDF file; the allowed dataset must have no more than two dimensions;
- **f\_HDF5Read\_FGDi**, used to read a subset of a three-dimensional dataset within a specified group, within the HDF file; the two-dimensional matrix read into Mathcad's workspace memory is identified by an index;



- `f_HDF5Read_FGDA`, used to read a subset's specific attribute 1.13.

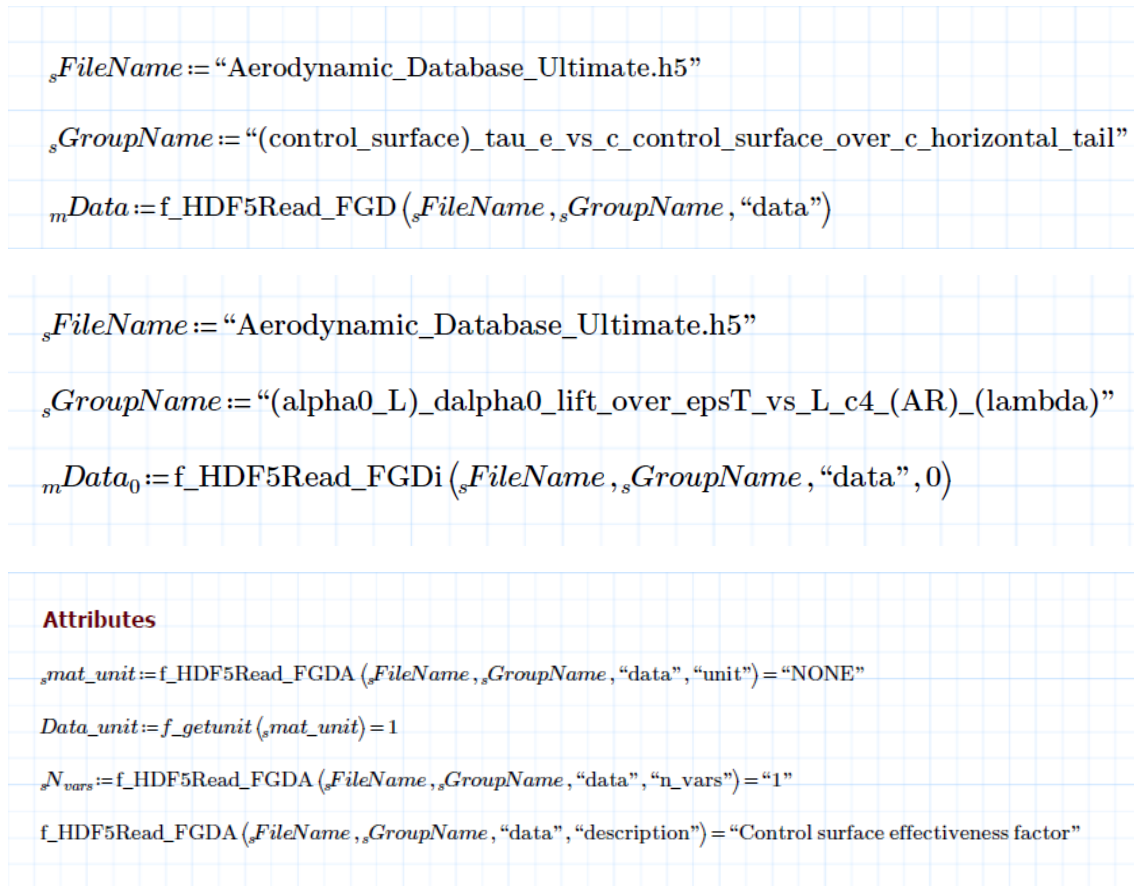


**Figure 1.13** Screenshots of the HDFView software.

Furthermore, in order to deal with non dimensional numbers in following interpolation calculations, it has been necessary to create another function called `f_getunit(strUnit)`. This function has as argument a character string. This string has been read precedently by `f_HDF5Read_FGDA`. Dependently from the string value, it returns a numerical value as shown in figure 1.14.

```

f_getunit(strUnit) :=
  if strUnit = "NONE"
    Out ← 1
  if strUnit = "MT"
    Out ← 1 m
  if strUnit = "FT"
    Out ← 1 ft
  if strUnit = "DEG"
    Out ← 1 deg
  if strUnit = "RAD"
    Out ← 1 rad
  if strUnit = "(DEG)^-1"
    Out ←  $\frac{1}{deg}$ 
  if strUnit = "(RAD)^-1"
    Out ←  $\frac{1}{rad}$ 
  if strUnit = "(DEG)^-2"
    Out ←  $\frac{1}{(deg)^2}$ 
  if strUnit = "(RAD)^-2"
    Out ←  $\frac{1}{(rad)^2}$ 
  if strUnit = "(RAD*DEG)^-1"
    Out ←  $\frac{1}{(rad \cdot deg)}$ 
  return Out

```

Figure 1.14 Screenshots of the HDFView software.

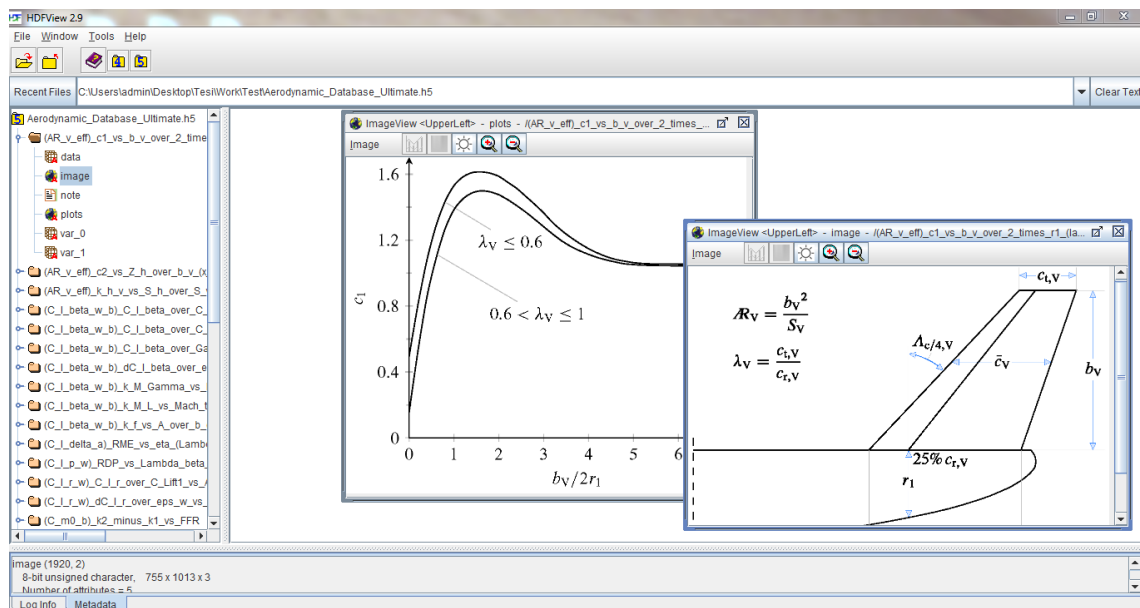
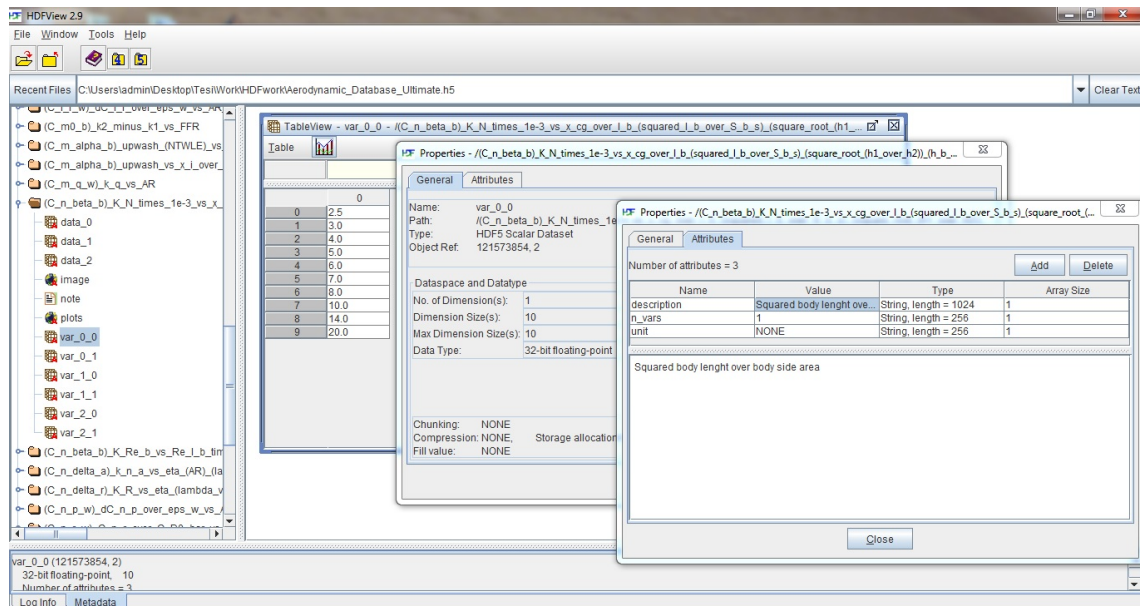
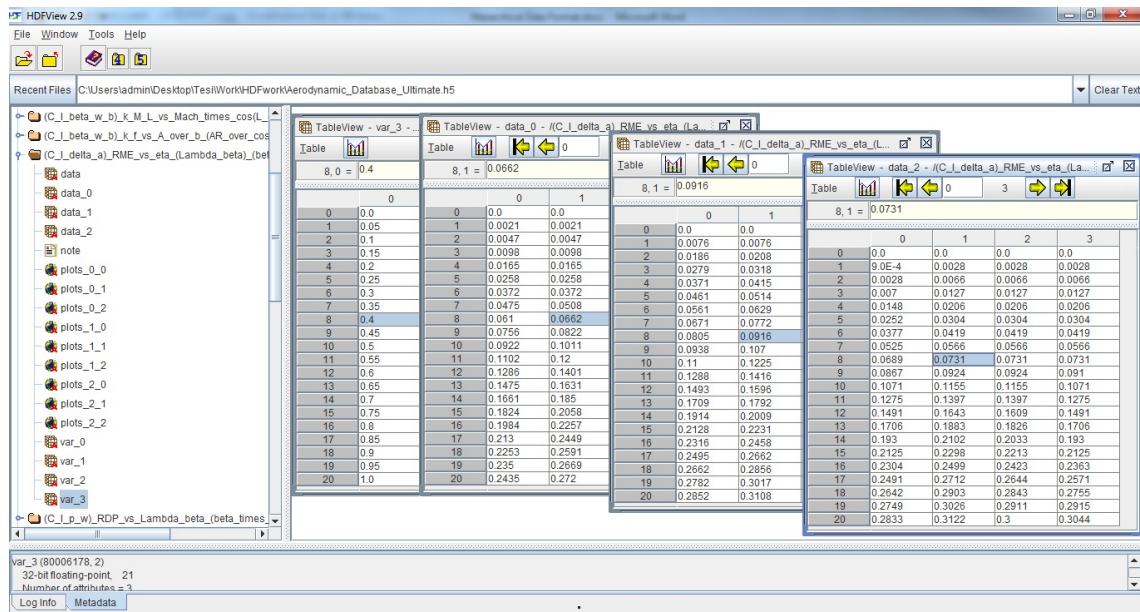


Figure 1.15 Screenshots of the HDFView software.



---

## REVIEW OF BASIC CONCEPTS OF AERODYNAMIC MODELING

---

The final aim of this chapter is showing the formulas and methods used to evaluate effectively the aerodynamic coefficients with regard to the aircraft as a whole. The calculation formulas are mostly based on the well known USAF DATCOM [2]. In particular, both for the specific formulations and for the symbols, we have used a single reference, namely the textbook by Napolitano [1].

In the following we will recall some of the most important formulas of Aircraft Stability and Control. These assume the validity of the superposition principle and express all quantities referred to the aircraft as a sum of a number of contributions. Each aerodynamic coefficient is computed first evaluating the contribution due to each part taken singularly; then the extra contribution due to aerodynamic interferences are estimated; finally, all contributions are summed up.

From now on, all angles are assumed to be in radian. Hence all the angular gradients will be evaluated in  $rad^{-1}$

### 2.1 Wing Related Parameters

In the following section we will show all formula and methods implemented in the wing-related Mathcad projects located in the file wing of Mathcad.

#### 2.1.1 Geometrical Data

Wing related data are taken from technical drawings or reports. These documents assume the profile near the wing-fuselage bond as the “root” profile. Hence, in the following linear approximations, all parameter related to “root” refers to the profile next to the wing-fuselage joint.

*Remark:* from now on all wing-related parameters refer to the ones of the equivalent

wing.

$$c(x) = c_0 + \frac{c_t - c_0}{\frac{b}{2}} \cdot x \quad (2.1)$$

$$C_{\ell_\alpha}(x) = C_{\ell_{\alpha_r}} + \frac{C_{\ell_{\alpha_t}} - C_{\ell_{\alpha_r}}}{\frac{b}{2} - \frac{d_B}{2}} \cdot \left(x - \frac{d_B}{2}\right) \quad (2.2)$$

$$C_{m_{ac}}(x) = C_{m_{ac_r}} + \frac{C_{m_{ac_t}} - C_{m_{ac_r}}}{\frac{b}{2} - \frac{d_B}{2}} \cdot \left(x - \frac{d_B}{2}\right) \quad (2.3)$$

$$\alpha_{0\ell}(x) = \alpha_{0\ell_r} + \frac{\alpha_{0\ell_t} - \alpha_{0\ell_r}}{\frac{b}{2} - \frac{d_B}{2}} \cdot \left(x - \frac{d_B}{2}\right) \quad (2.4)$$

$$\bar{x}_{ac}(x) = \bar{x}_{ac_r} + \frac{\bar{x}_{ac_t} - \bar{x}_{ac_r}}{\frac{b}{2} - \frac{d_B}{2}} \cdot \left(x - \frac{d_B}{2}\right) \quad (2.5)$$

$$\varepsilon(x) = \varepsilon_r + \frac{\varepsilon_t - \varepsilon_r}{\frac{b}{2} - \frac{d_B}{2}} \cdot \left(x - \frac{d_B}{2}\right) \quad (2.6)$$

$$M_{cr}(x) = M_{cr} + \frac{M_{cr_{2d_t}} - M_{cr_{2d_r}}}{\frac{b}{2} - \frac{d_B}{2}} \cdot \left(x - \frac{d_B}{2}\right) \quad (2.7)$$

Whereas in all other formulas we consider “root” profile the one lengthened to the fuselage centre line. This can be evaluated with ease using the linear functions computed in  $x = 0$ . From now on  $c_r = c(0)$ , namely the root chord will be referred to the profile at the fuselage centre line. And MAC will stand for *Mean Aerodynamic Chord*.

In the figure 2.1 on the facing page are shows some characteristic parameters of nonstraight wing planform.

$$\lambda = \frac{c_t}{c_r} \quad (2.8)$$

$$S = \frac{b}{2} c_r (1 + \lambda) \quad (2.9)$$

$$\mathcal{R} = \frac{b^2}{S} \quad (2.10)$$

$$MAC = \frac{2}{3} c_r \frac{1 + \lambda + \lambda^2}{1 + \lambda} \quad (2.11)$$

$$y_{MAC} = \frac{b}{6} \frac{1 + 2\lambda}{1 + \lambda} \quad (2.12)$$

$$x_{MAC} = y_{MAC} \tan \Lambda_{LE} \quad (2.13)$$

$$S_{\text{Control Surface}} = S \frac{\eta_o - \eta_i}{1 + \lambda} \left[ 2 - (1 - \lambda)(\eta_i + \eta_o) \right] \quad (2.14)$$

$$\Lambda(x) = \arctan \left[ \tan \Lambda_{LE} - \frac{4x(1 - \lambda)}{\mathcal{R}(1 + \lambda)} \right] \quad (2.15)$$

Arm needed for computing the Pitching Moment Coefficient about the Aerodynamic

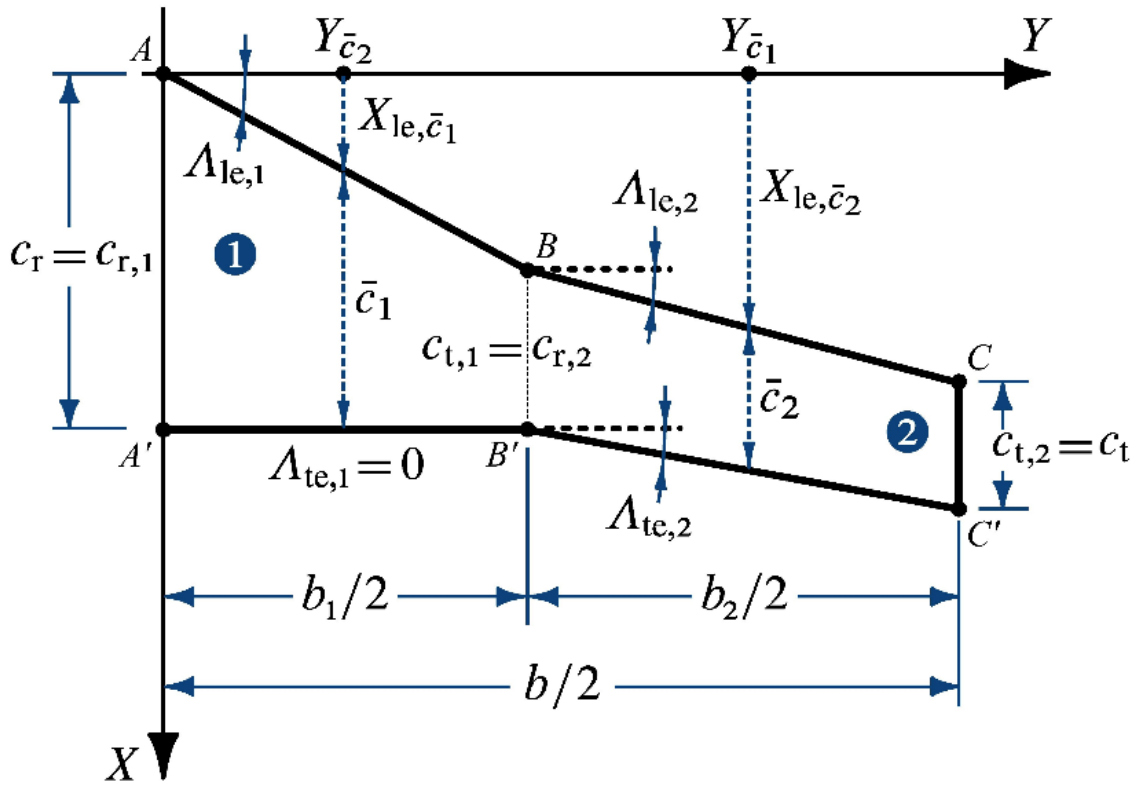


Figure 2.1 Generic Nonstraight Wing Planform

Centre:

$$X_1(x) = \tan(\Lambda_{LE})x + \bar{x}_{ac}(x)c(x) - \left[ x_{MAC} + x_{ac}(y_{MAC})MAC \right] \quad (2.16)$$

### 2.1.2 Aerodynamic Parameters

$$\alpha_{0L} = \frac{2}{S} \int_0^{\frac{b}{2}} c(x) \left[ \alpha_{0\ell}(x) - \varepsilon(x) \right] dx \quad (2.17)$$

$$\alpha_{0L_{Control\ Surface}} = \alpha_{0L} + \frac{S_{Control\ Surface}}{S} \Delta\alpha_{0\ell} \quad (2.18)$$

$$M_{cr3D} = \frac{M_{cr2D}(x_{MAC})}{\cos \Lambda_{LE}} \quad (2.19)$$

In order to compute accurately the Lift Coefficient Gradient we selected two different methods depending on both flight conditions and aircraft geometry. In details when:

- 1  $M_\infty < M_{cr3D}$
- 2  $\Lambda_{LE} < 32^\circ$
- 3  $0.4 < \lambda < 1$
- 4  $3 < \mathcal{R} < 8$

*Remark:*  $M_{cr3D}$  is evaluated at the MAC.

$$C_{L\alpha} = \frac{2\pi \mathcal{R}}{2 + \sqrt{\left[ \frac{\mathcal{R}^2(1 - M^2)}{k_1^2} \left( 1 + \frac{\tan^2 \Lambda(0.5)}{1 - M^2} \right) + 4 \right]}} \quad (2.20)$$

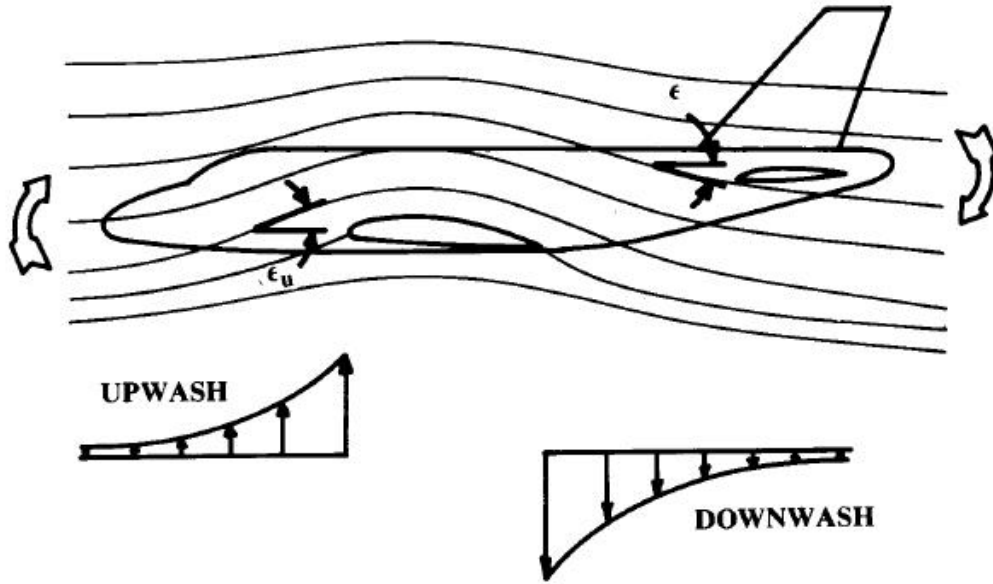


Figure 2.2 Downwash Effect

where  $k_1$  is a function of  $\mathcal{R}$  computed as shown:

$$k_1 = \begin{cases} 1 + \frac{\mathcal{R}(1.87 - 0.000233\Lambda_{LE})}{100}, & \text{if } \mathcal{R} < 4 \\ 1 + \frac{(8.2 - 2.3\Lambda_{LE}) - \mathcal{R}(0.22 - 0.153\Lambda_{LE})}{100}, & \text{if } \mathcal{R} \geq 4 \end{cases} \quad (2.21)$$

Whereas, if the above conditions 1) to 4) are not fulfilled:

$$C_{L\alpha} = \frac{C_{\ell_\alpha}(y_{MAC}) \cos \Lambda_{LE}}{\sqrt{1 - (M_\infty \cos \Lambda_{LE})^2 + \left(C_{\ell_\alpha}(y_{MAC}) \frac{\cos \Lambda_{LE}}{\pi \mathcal{R}}\right)^2 + C_{\ell_\alpha}(y_{MAC}) \frac{\cos \Lambda_{LE}}{\pi \mathcal{R}}}} \quad (2.22)$$

where  $C_{\ell_\alpha}$  is a function evaluated at  $x_{MAC}$ .

$$C_{M_{ac}} = \frac{2}{S \cdot MAC} \left\{ \int_0^{\frac{b}{2}} C_{m_{ac}}(x) c(x)^2 dx + \pi \int_0^{\frac{b}{2}} [\alpha_{0L} + \varepsilon(x) - \alpha_{0\ell}(x)] c(x) X_1(x) dx \right\} \quad (2.23)$$

### 2.1.3 Downwash

An important longitudinal aerodynamic effect is the so-called downwash effect. In general, this effect can be considered to be an aerodynamic *interference* generated by the wing on the horizontal tail due to the system of vortices created by the wing itself, see figure 2.2.

Suppose we can approximate the downwash function using Taylor's series ended at first grade accuracy. Hence:

$$\varepsilon(M) = \varepsilon_0 + \frac{\partial \varepsilon}{\partial \alpha}(M) \quad (2.24)$$



where  $\frac{\partial \varepsilon}{\partial \alpha}$  is a given function of the Mach number:

$$\left( \frac{\partial \varepsilon}{\partial \alpha} \right) = f(Mach, m, r, \Lambda_L E, \lambda, AR)$$

$$\left. \frac{\partial \varepsilon}{\partial \alpha} \right|_M = \left. \frac{\partial \varepsilon}{\partial \alpha} \right|_{M=0} \sqrt{1 - M^2} \quad (2.25)$$

in which the downwash gradient at  $M = 0$  is given by the following semi - empirical formula:

$$\left. \frac{\partial \varepsilon}{\partial \alpha} \right|_{M=0} = 4.44 \left( K_{AR} K_{\lambda} K_{mr} \sqrt{\cos \Lambda_{0.25}} \right)^{1.19} \quad (2.26)$$

The coefficients in the above equation can be computed as follow:

$$K_{AR} = \frac{1}{AR} - \frac{1}{1 + (AR)^{1.7}}, \quad K_{\lambda} = \frac{10 - 3\lambda}{7}, \quad K_{mr} = \frac{1 - \frac{m_{WH}}{2}}{(r_{WH})^{0.33}}$$

Let us consider two important geometrical parameters to estimate the coefficients needed to compute  $K_{mr}$ :

$x_{W,H}$  - the horizontal distance between wing and horizontal tail LE.

$z_{W,H}$  - the vertical distance between wing and horizontal tail root chord.

hence, we can define:

$$X_{ac_{W,H}} = x_{W,H} + (y_{MAC,H} + \bar{x}_{ac,H} MAC_H) - (y_{MAC,W} + \bar{x}_{ac,W} MAC_W) \quad (2.27)$$

$$Z_{ac_{W,H}} = z_{W,H} + y_{MAC,H} \tan \Gamma_H - y_{MAC,W} \tan \Gamma_W \quad (2.28)$$

and eventually:

$$m_{WH} = 2 \frac{Z_{ac_{W,H}}}{b} \quad (2.29)$$

$$r_{WH} = 2 \frac{X_{ac_{W,H}}}{b} \quad (2.30)$$

## 2.2 Horizontal Tail Related Parameters

To compute all parameters needed with regard to the Horizontal Tail (HT), see Section 3.3 on page 41 and 3.4 on page 42. Please notice, that in this case the root profile related parameters are always referred to the fuselage centre line. This means a general linear approximation can be:

$$c(x) = c_r + \frac{2}{b} (c_t - c_r) x \quad (2.31)$$

Moreover, the HT is assumed to be a non-cranked wing, therefore it will not be processed using the procedure *Equivalent Surface Function*.

## 2.3 Longitudinal Stability

In this section we will show all formula and methods implemented in the MArYsa software used to compute the longitudinal coefficients, namely *Longitudinal Flight Coefficients* and *Multhopp*. The algorithms are located in the folder *Longitudinal Calculation*.

### 2.3.1 General Parameters

$$\alpha_{WB} = \alpha_B + i_W - \alpha_{0L,W} \quad (2.32)$$

$$\alpha_H = \alpha_{WB} \left( 1 - \frac{\partial \varepsilon}{\partial \alpha} \Big|_{M_\infty} \right) \quad (2.33)$$

$$V_H = \eta_H \frac{S_H}{S_W} \quad (2.34)$$

$$c_{\tau_e} = \frac{c_{H_e}}{c_{H_r}} \quad (2.35)$$

$$e = \frac{1.1 C_{L_{\alpha,W}}}{R C_{L_{\alpha,W}} + (1 - R) \pi \mathcal{R}_W} \quad (2.36)$$

$$R = 0.0004 \lambda_e^3 - 0.008 \lambda_e^2 + 0.0501 \lambda_e + 0.8642 \quad (2.37)$$

$$\lambda_e = \frac{\mathcal{R}_W \lambda_W}{\cos \Lambda_{W,LE}} \quad (2.38)$$

$$\text{FFR} = \frac{l_B}{d_B} \quad (2.39)$$

Distance between wing TE and HT aerodynamic centre

$$l_{WTE,Hac} = x_{W,H} - c_{W,r} + (x_{MAC_H} + MAC_H \xi_{ac,H}) \quad (2.40)$$

Distance between wing and HT aerodynamic centre

$$l_{Wac,Hac} = x_{W,H} + (x_{MAC_H} + MAC_H \xi_{ac,H}) \quad (2.41)$$

### 2.3.2 Fuselage Contribution evaluated using Multhopp's Method

$$C_{M_{0,B}} = \frac{\pi(K_2 - K_1)}{2S_W MAC_W} \sum_{k=0}^{n_0-2} \left[ W_{B,k}^2 (-i_W + \alpha_{0L,W} + i_{cl,k}) \right] \Delta x \quad (2.42)$$

where  $K_2 - K_1$  is given by Figure 2.3 on the next page. The above formula is taken from the textbook by Pamadi [6].

$$C_{M_{\alpha,B}} = \frac{\pi}{2S_W MAC_W} \left\{ \sum_{k=0}^{n_1-2} W_{B,k}^2 \left[ \left( \frac{\partial \varepsilon}{\partial \alpha} (M_\infty) \right)_u + 1 \right] \Delta x_1 + \sum_{k=0}^{n_2-2} W_{B,k}^2 \left[ \left( \frac{\partial \varepsilon}{\partial \alpha} (M_\infty) \right)_d + 1 \right] \Delta x_2 \right\} \quad (2.43)$$

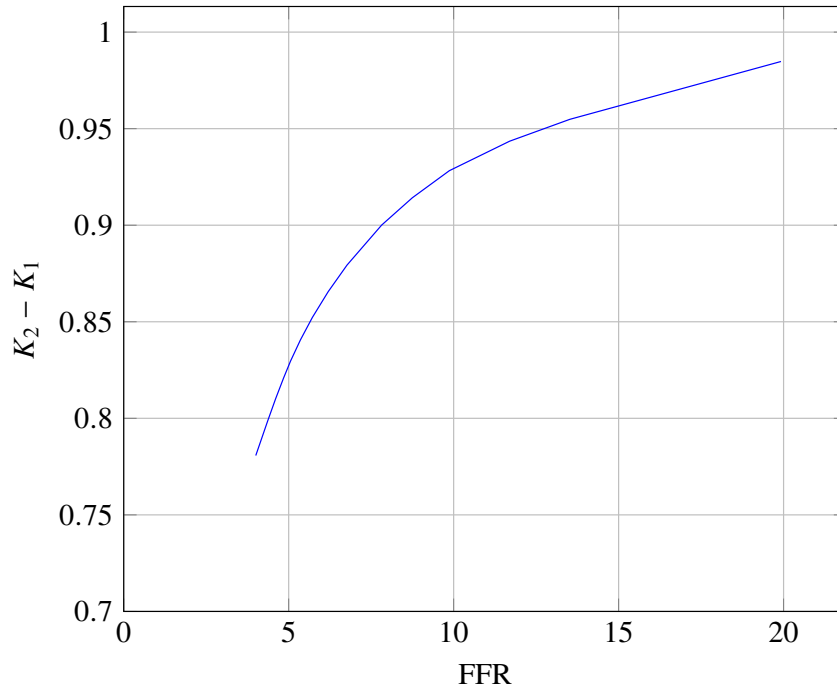


**Figure 2.3** Fuselage Apparent Mass Coefficient (function of the Fuselage Fitness Ratio – FFR).

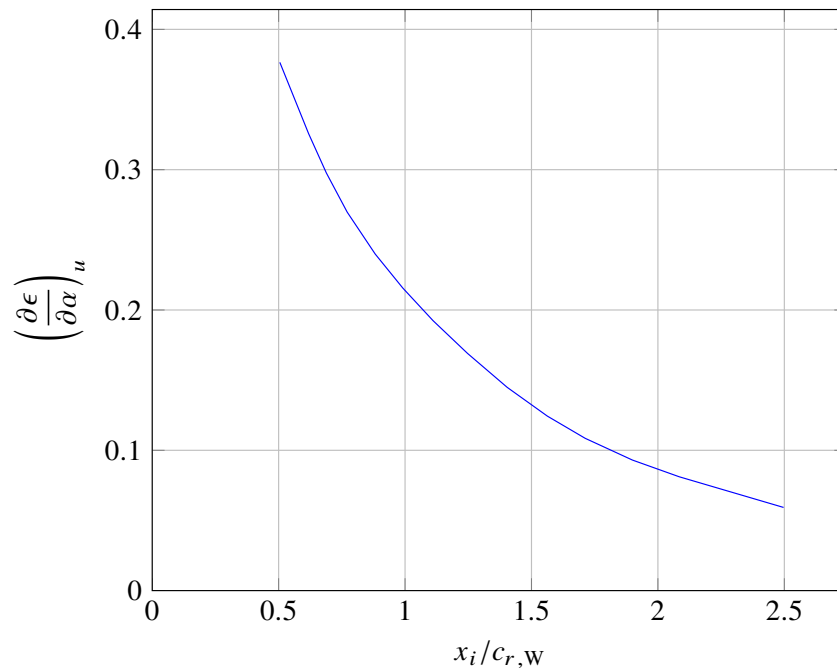


**Figure 2.4** Upwash for Front Fuselage Sections.

where  $(\partial \varepsilon / \partial \alpha)_{M_\infty}_u$  is evaluated from Figure 2.4 for front fuselage sections and by Figure 2.5 on the next page for the ones next to wing LE.

Whereas  $(\partial \varepsilon / \partial \alpha)_{M_\infty}_d$  is evaluated as follow:

$$\left( \frac{\partial \varepsilon}{\partial \alpha} M_\infty \right)_d + 1 = \frac{x_i}{l_{WTE,Hac}} \left( 1 - \frac{\partial \varepsilon}{\partial \alpha} M_\infty \right) \quad (2.44)$$

where  $x_i$  is the distance between the fuselage section centroid and the wing TE. The

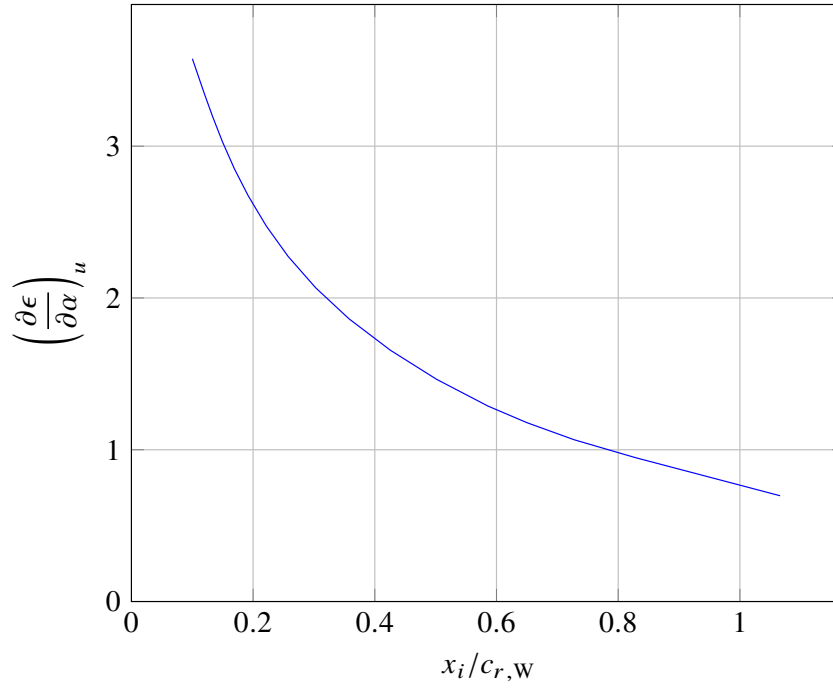


**Figure 2.5** Upwash for Fuselage Sections next to Wing LE - NTWLE.

following is the Multhopp formula for the gradient of the pitching moment coefficient

$$C_{M_{\alpha B, \text{Multhopp}}} = \frac{\pi}{2S_W MAC_W} \left\{ \sum_{k=0}^{n_1-2} W_{B_k}^2 \left[ \left( \frac{\partial \varepsilon}{\partial \alpha} M_\infty \right)_u + 1 \right] \Delta x_1 + \sum_{k=0}^{n_2-2} W_{B_k}^2 \left[ \left( \frac{\partial \varepsilon}{\partial \alpha} M_\infty \right)_d + 1 \right] \Delta x_2 \right\} \quad (2.45)$$

where the upwash gradient is computed as above while the downwash gradient is evaluated considering

### 2.3.3 Aerodynamic Centre

$$\xi_{ac,w} = K_1 \left( \frac{x_{ac,w}}{c_{r,w}} - K_2 \right) \quad (2.46)$$

$$\xi_{wac,hac} = \frac{l_{wac,hac}}{MAC_w} \quad (2.47)$$

$$\Delta \xi_{ac,wb} = -\frac{C_{M_{\alpha,b}}}{C_{L_{\alpha,w}}} \quad (2.48)$$

The empirical coefficients  $K_1$ ,  $x_{ac,w}/c_{r,w}$  and  $K_2$  needed to compute  $\xi_{ac,w}$  are taken from charts of Figure 2.6 on the facing page, 2.7 on page 34, and 2.8 on page 35 respectively.

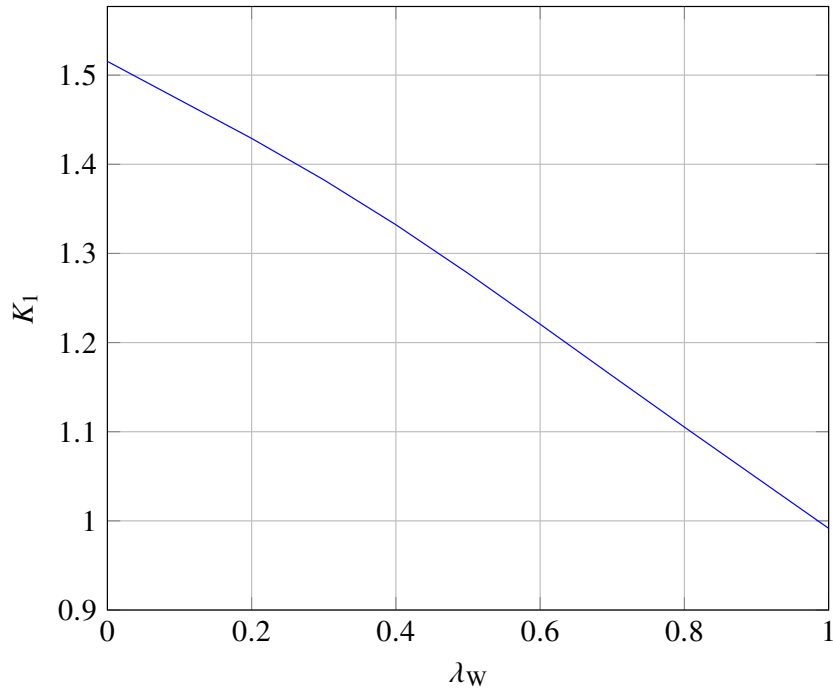


**Figure 2.6**  $K_1$  Coefficient for the Calculation of  $\xi_{ac,W}$ .

$$\begin{aligned} \Delta \xi_{ac, WB, Multihopp} = \frac{\pi}{9S_W MAC_W} & \left\{ \sum_{k=0}^{n_1-2} W_{B_k}^2 \left[ \left( \frac{\partial \varepsilon}{\partial \alpha}(M_\infty) \right)_u + 1 \right] \Delta x_1 \right. \\ & + \sum_{k=0}^{n_W-2} W_{B_k}^2 \left[ \left( \frac{\partial \varepsilon}{\partial \alpha}(M_\infty) \right)_d + 1 \right] \Delta x_W \\ & \left. + \sum_{k=0}^{n_2-2} W_{B_k}^2 \left[ \left( \frac{\partial \varepsilon}{\partial \alpha}(M_\infty) \right)_d + 1 \right] \Delta x_2 \right\} \quad (2.49) \end{aligned}$$

where the upwash gradient is computed as above while the downwash gradient is evaluated considering  $\partial \varepsilon / \partial \alpha|_{M_\infty}$  at  $m_{W,H} = 0$

$$\xi_{ac, WB} = \xi_{ac, W} + \Delta \xi_{ac, WB} \quad (2.50)$$

$$\xi_{ac, WB, Multihopp} = \xi_{ac, W} + \Delta \xi_{ac, WB, Multihopp} \quad (2.51)$$

### 2.3.4 Lift Coefficients

$$C_{L\alpha, WB} = K_{WB} C_{L\alpha, W} \quad (2.52)$$

$$K_{WB} = 1 + 0.025 \left( \frac{d_B}{b_W} \right) - 0.25 \left( \frac{d_B}{b_W} \right)^2 \quad (2.53)$$

$$C_{L0, WB} = C_{L\alpha, WB} (i_W - \alpha_{0L, W}) \quad (2.54)$$

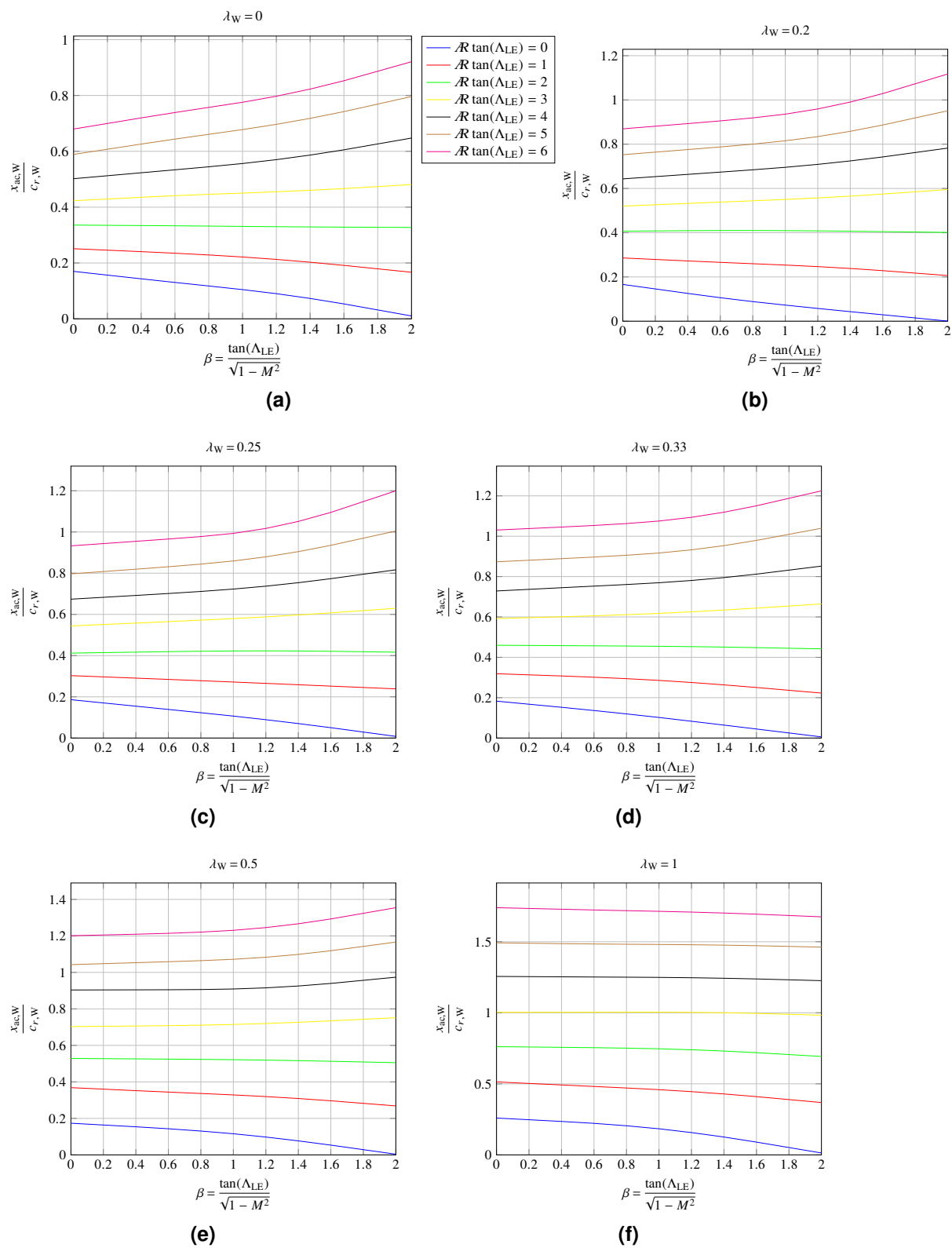


**Figure 2.7**  $\frac{X_{ac,W}}{C_{r,W}}$  for different airspeed.

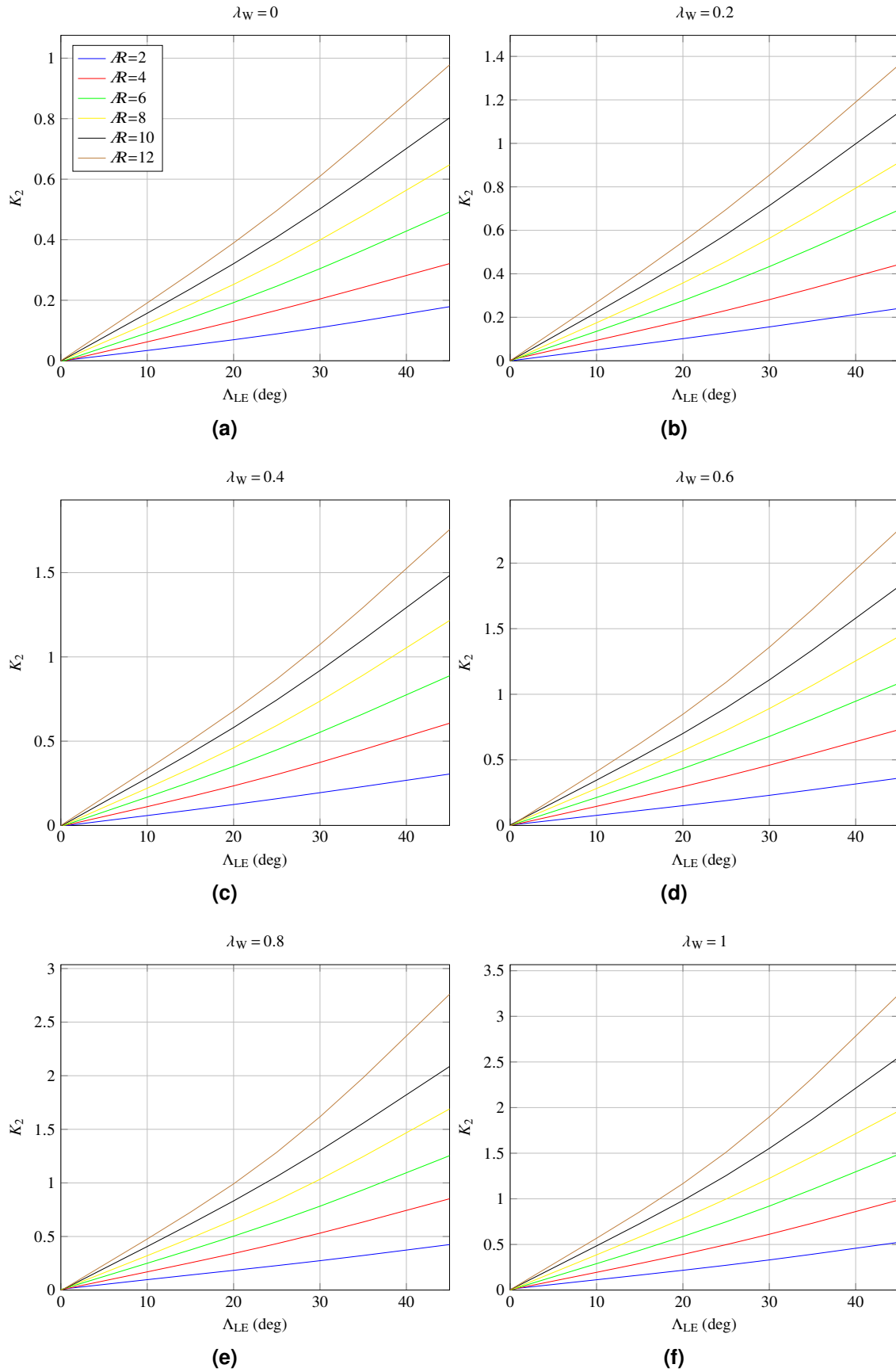


**Figure 2.8**  $K_2$  Coefficient for the Calculation of  $\xi_{ac,w}$ .

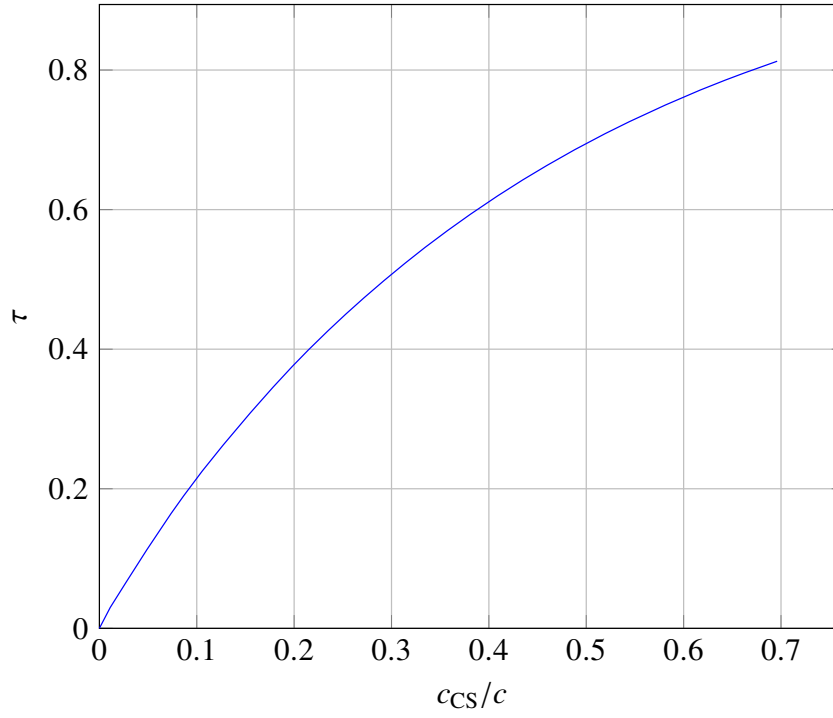


**Figure 2.9** Control Surface Effectiveness against  $\frac{c_{CS}}{c}$

$$C_{L_{0,H}} = C_{L_{\alpha,H}} (i_W - \alpha_{0L,W}) \left( 1 - \frac{\partial \varepsilon}{\partial \alpha} M_\infty \right) \quad (2.55)$$

$$C_{L_0} = C_{L_{0,WB}} - C_{L_{\alpha,H}} V_H \varepsilon_0 + C_{L_{0,H}} \quad (2.56)$$

$$C_{L_\alpha} = \left( 1 - \frac{\partial \varepsilon}{\partial \alpha} M_\infty \right) C_{L_{\alpha,H}} V_H + C_{L_{\alpha,WB}} \quad (2.57)$$

$$C_{L_{i_H}} = C_{L_{\alpha,H}} V_H \quad (2.58)$$

$$C_{L_{\delta_e}} = C_{L_{\alpha,H}} V_H \tau_e \quad (2.59)$$

where  $\tau_e$  is a function of  $c_{\tau_e}$  taken from Figure 2.9.

### 2.3.5 Coefficients at Stick-Fixed Conditions

$$C_{M_{0,WB}} = C_{M_{ac,W}} + C_{M_{0,B}} \quad (2.60)$$

$$C_{M_0} = C_{M_{0,WB}} + C_{L_{0,WB}} (\xi_{CG} - \xi_{ac,WB}) + C_{L_{\alpha,H}} V_H \varepsilon_0 (\xi_{Wac,Hac} - \xi_{CG}) \quad (2.61)$$

$$C_{M_\alpha} = C_{L_{\alpha,WB}} (\xi_{CG} - \xi_{ac,WB}) - C_{L_{\alpha,H}} V_H (\xi_{Wac,Hac} - \xi_{CG}) \left( 1 - \frac{\partial \varepsilon}{\partial \alpha} M_\infty \right) \quad (2.62)$$

$$C_{M_{i_H}} = -C_{L_{\alpha,H}} V_H (\xi_{Wac,Hac} - \xi_{CG}) \quad (2.63)$$

$$C_{M_{\delta_e}} = C_{M_{i_H}} \tau_e \quad (2.64)$$



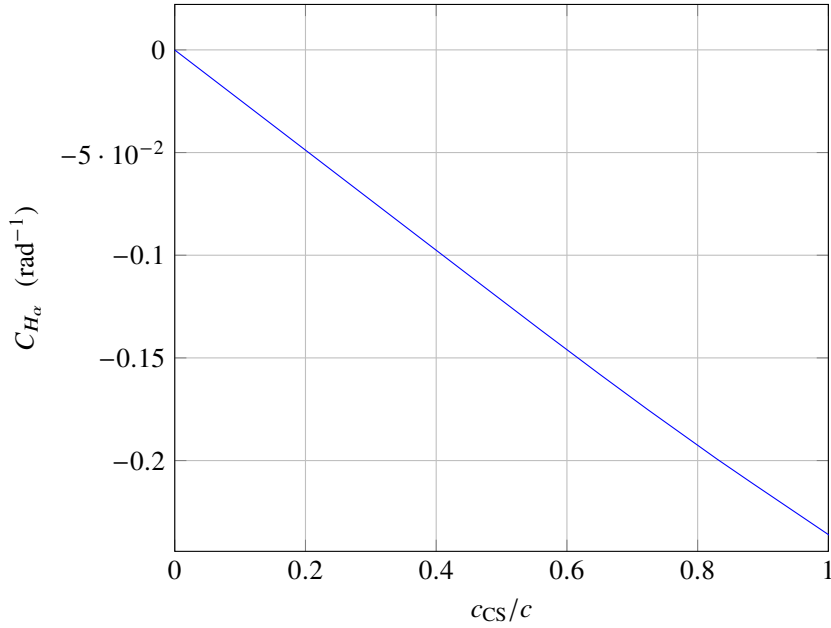


**Figure 2.10** Hinge Moment Coefficient Derivate with regard to  $\alpha$ .

$$\delta_e = -\frac{C_{M_0} + C_{M_\alpha}\alpha_{WB} + C_{M_{i_H}}i_H}{C_{M_{\delta_e}}} \quad (2.65)$$

$$i_H = -\frac{C_{M_0} + C_{M_\alpha}\alpha_{WB} + C_{M_{\delta_e}}\delta_e}{C_{M_{i_H}}} \quad (2.66)$$

The procedure is programmed so if  $i_H$  is given as input, it yields  $\delta_e$  and viceversa. In the input files if the angle has to be calculated its value must be 999. Once evaluated all parameters, we can compute the neutral point:

$$\xi_N = \frac{\left[ \frac{\xi_{ac,WB}}{\xi_{Wac,Hac}} + \frac{C_{L_{\alpha,H}}}{C_{L_{\alpha,WB}}} V_H \left( 1 - \frac{\partial \varepsilon}{\partial \alpha} M_\infty \right) \right] \xi_{Wac,Hac}}{1 + \frac{C_{L_{\alpha,H}}}{C_{L_{\alpha,WB}}} V_H \left( 1 - \frac{\partial \varepsilon}{\partial \alpha} M_\infty \right)} \quad (2.67)$$

### 2.3.6 Stick-Free Conditions

Shape Factor:

$$F = 1 - \tau_e \frac{C_{H_{e\alpha}}}{C_{H_{\delta_e\alpha}}} \quad (2.68)$$

where  $C_{H_{e\alpha}}$  and  $C_{H_{\delta_e\alpha}}$  are given by experimental data on Figure 2.10 and 2.11 on the next page respectively.

All the coefficients are evaluated as in the Stick-Fixed Conditions 2.3.5 with the only exception for the terms due to the horizontal tail which are multiplied by  $F$  (see formula 2.68). Therefore, omitting formulas that remain unchanged:

$$C_{M_0} = C_{M_{0,WB}} + C_{L_{0,WB}}(\xi_{CG} - \xi_{ac,WB}) + C_{L_{\alpha,H}} V_H \varepsilon_0 (\xi_{Wac,Hac} - \xi_{CG}) F \quad (2.69)$$

$$C_{M_\alpha} = C_{L_{\alpha,WB}}(\xi_{CG} - \xi_{ac,WB}) - C_{L_{\alpha,H}} V_H (\xi_{Wac,Hac} - \xi_{CG}) \left( 1 - \frac{\partial \varepsilon}{\partial \alpha} M_\infty \right) F \quad (2.70)$$

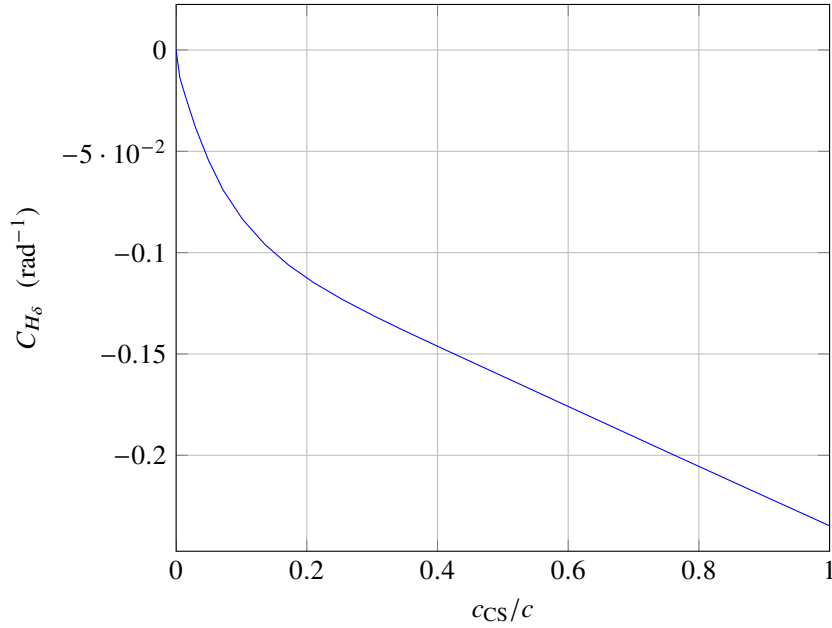


**Figure 2.11** Hinge Moment Coefficient Derivate with regard to  $\delta$ .

$$C_{M_{i_H}} = -C_{L_{\alpha,H}} V_H (\xi_{Wac,Hac} - \xi_{CG}) F \quad (2.71)$$

$$\alpha_{free} = -\frac{C_{M_0} + C_{M_{i_H}} i_H}{C_{M_{\alpha}}} \quad (2.72)$$

$$\alpha_{H,free} = \alpha_{free} \left( 1 - \frac{\partial \varepsilon}{\partial \alpha} M_{\infty} \right) - \varepsilon_0 + i_H \quad (2.73)$$

$$\delta_{e,free} = -\frac{C_{M_0} + C_{M_{\alpha}} \alpha_{WB} + C_{M_{i_H}} i_H}{C_{M_{\delta_e}}} \quad (2.74)$$

Once evaluated all parameters, we can compute the neutral point:

$$\xi_N = \frac{\left[ \frac{\xi_{ac,WB}}{\xi_{Wac,Hac}} + \frac{C_{L_{\alpha,H}}}{C_{L_{\alpha,WB}}} V_H \left( 1 - \frac{\partial \varepsilon}{\partial \alpha} M_{\infty} \right) F \right] \xi_{Wac,Hac}}{1 + \frac{C_{L_{\alpha,H}}}{C_{L_{\alpha,WB}}} V_H \left( 1 - \frac{\partial \varepsilon}{\partial \alpha} M_{\infty} \right) F} \quad (2.75)$$

### 2.3.7 Total Lift and Drag Coefficients

Once chosen the flight conditions (whether fixed or free) and evaluated all parameters needed, the following relations can be always used:

$$C_L = C_{L_0} + C_{L_{\alpha}} \alpha_{WB} + C_{L_{\delta_e}} \delta_e + C_{L_{i_H}} i_H \quad (2.76)$$

$$C_D = C_{D_0} + \frac{C_L^2}{\pi \mathcal{R}_{We}} \quad (2.77)$$

$$C_{D_{\alpha}} = \frac{2 C_L C_{L_{\alpha}}}{\pi \mathcal{R}_{We}} \quad (2.78)$$

$$SSM = \xi_N - \xi_{CG} \quad (2.79)$$

# Chapter **3**

## NUMERICAL TEST SAMPLE ON BOEING 787 DREAMLINER

This chapter describes an applicative example of study about longitudinal stability of Boeing 787 Dreamliner, given by software MArYSA previously mentioned.

Calculated formula are came from Aircraft Dynamics: from Modeling to Simulation By Napolitano [1].



**Figure 3.1** Boeing 787 Dreamliner.



Figure 3.2 Wing of Boeing 787.

### 3.1 Boeing 787 Dreamliner

The Boeing 787 Dreamliner is a twin-engined aircraft with *wide-body* fuselage, used as airliner and worked out by the American Company Boeing, and assembled with several elements produced on commission in different countries of the world.

This aircraft, the first in the world airliners built with a lot of *carbon fibers*, we can find different models for instance one supplied by bio-fuels.

The Boeing 787 Dreamliner is the first airliner produced with high percentage of carbon fibers, over 50%. The fuselage of this aircraft is carbon fibers made, with some titanium parts to strengthen the structure, this represents an important change. The use of this material on a massive scale let save more 20% of the weight than a traditional aircraft with the same size, aluminium made.

Moreover the decrease in weight, with new motors and excellent aerodynamics allow the Boeing 787 Dreamliner to save a lot of fuel than the traditional airliners. This is the reason because many companies has chosen the 787 to change their fleet.

Besides the level of worsening of fuselage, caused by corrosion for an aluminium aircraft generally, is very low, this allows the aircraft to save money for both ordinary and emergency maintenance.

Another characteristic about this aircraft is *wing*, see figure 3.2, which is not only all out of carbon fiber but with high lengthening to cut down on lift-induced drag. This allows both take off and landing, and Boeing 787 will be able to land on very short landing strip.

An further special characteristic is aircraft productive process. Infact the fuselage structure is all out of only five pieces than joined together.

Instead the traditional productive process about aluminium aircraft deals some middle (ordinate ) structures which are generally little aluminium board covered. Producing fuselages with a little number of elements gives them more rigidity and resistance.

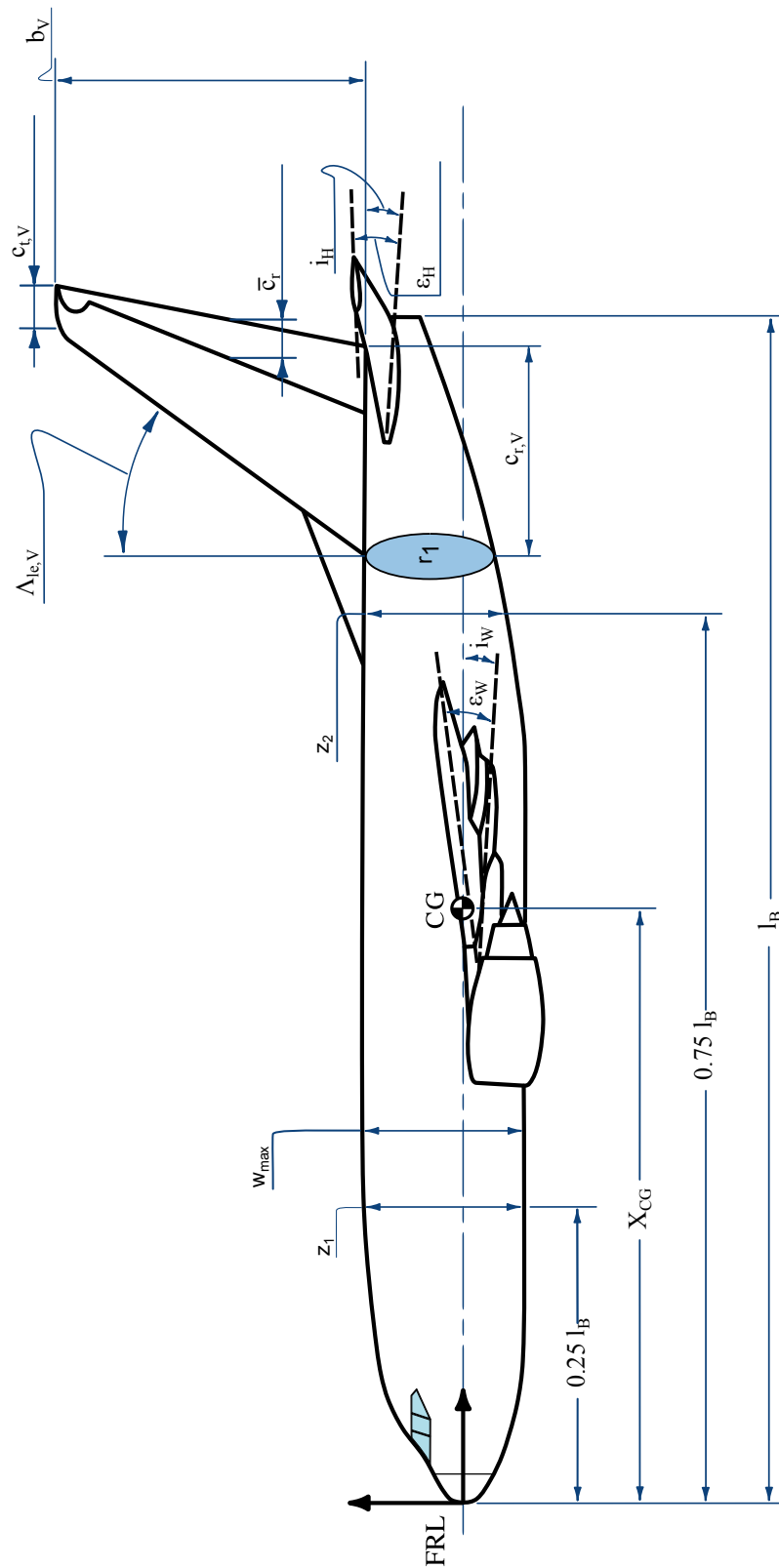


**Figure 3.3** Side View of Boeing 787.

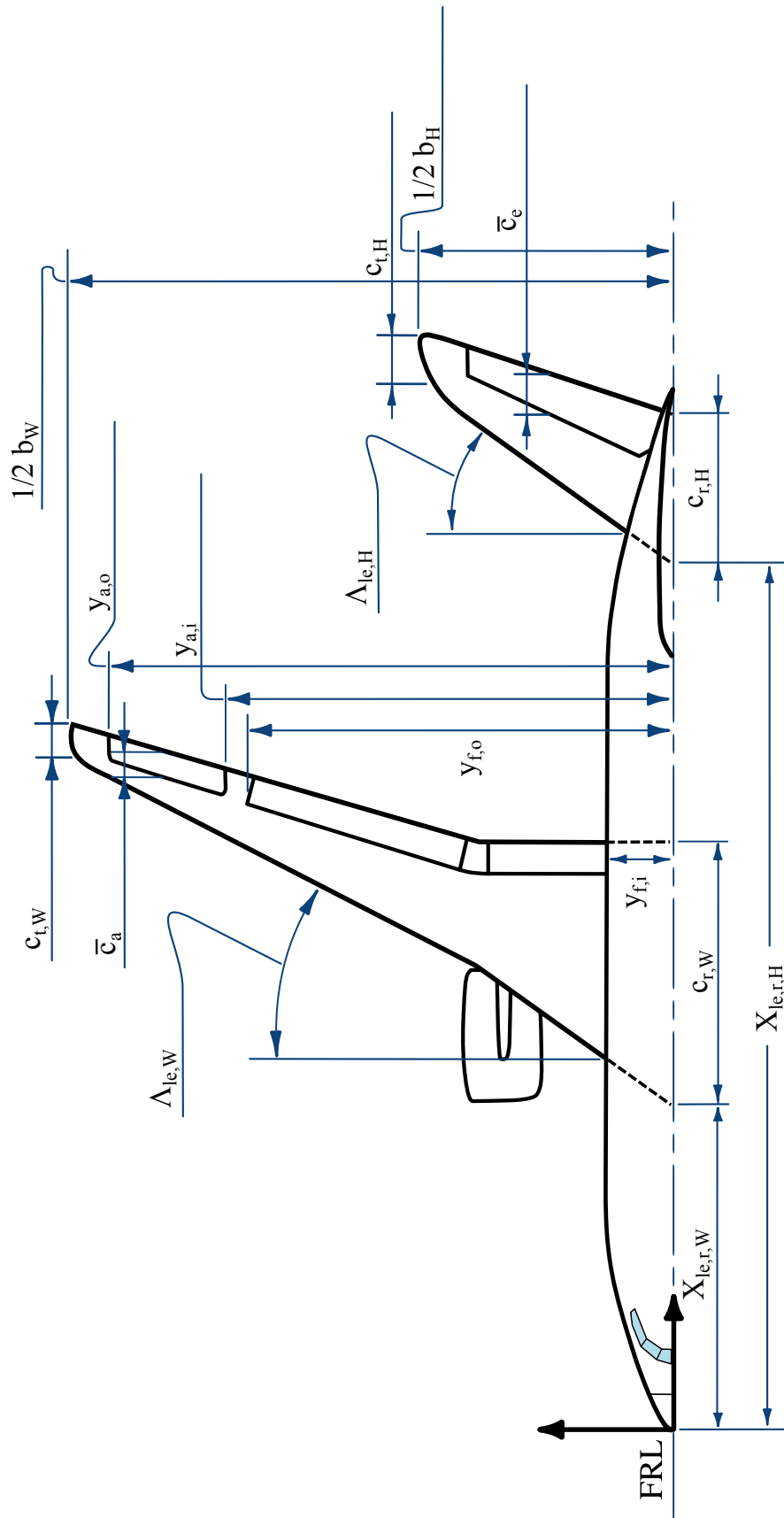


**Figure 3.4** Top View of Boeing 787.

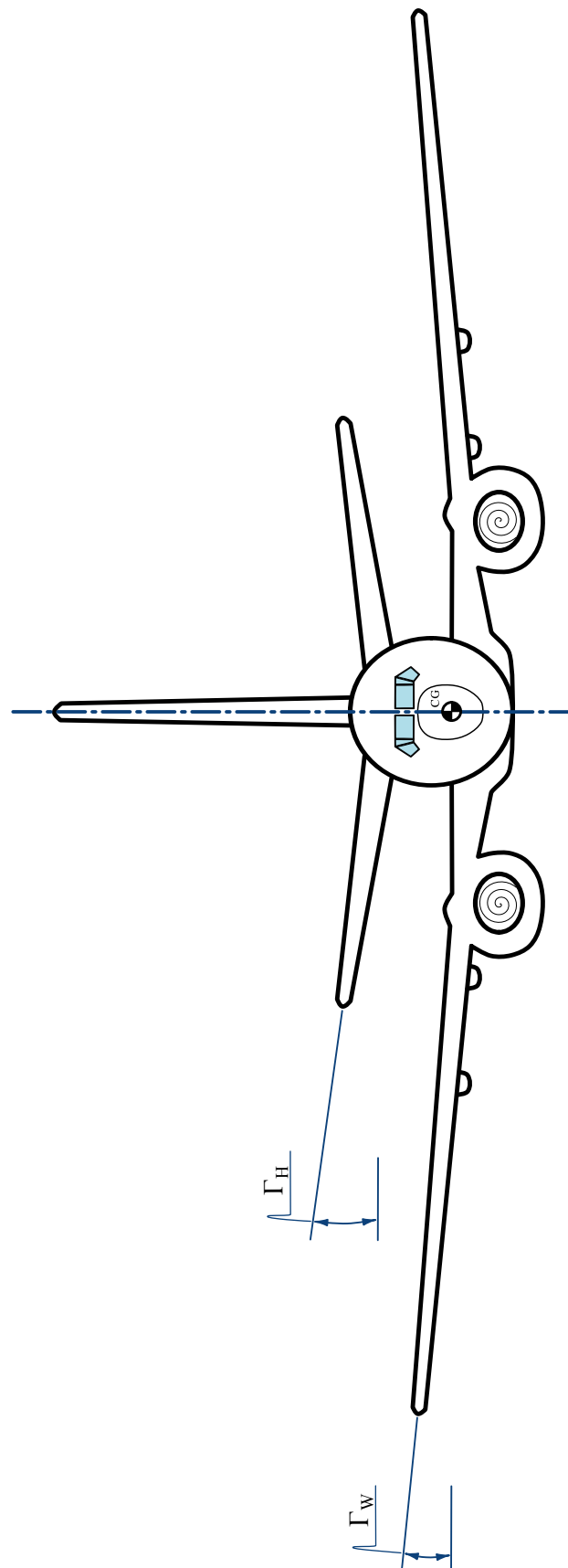


**Figure 3.5** Front View of Boeing 787.

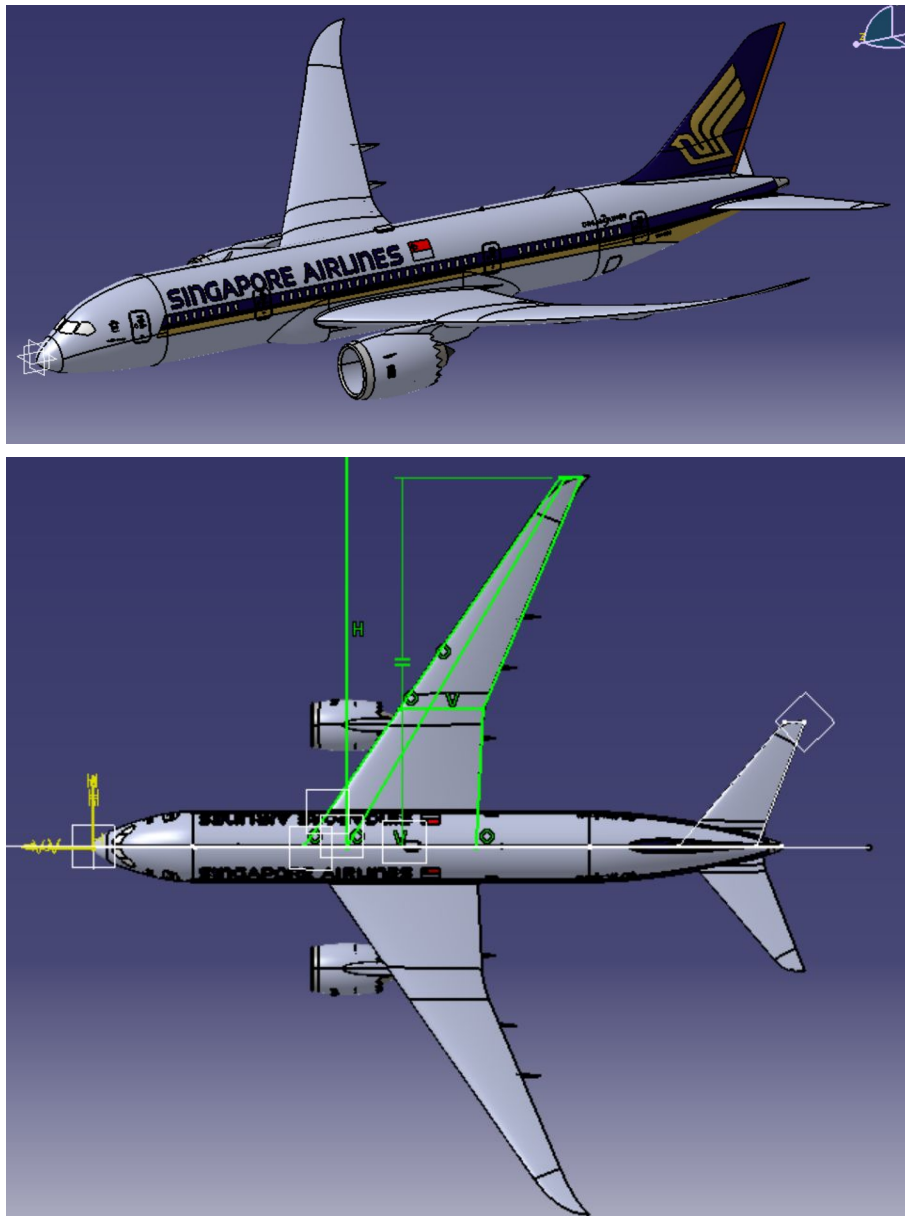


**Figure 3.6** Modeling of 787-Dreamliner with CatiaV5

## 3.2 Parameters research

The next schedule represent a set data based on use of software MArYSA whether straightly or not.

Geometric parameters are taken from use of a cad model Boeing 787 Dreamliner downloaded on web <http://grabcad.com/library/boeing-787-dreamliner>.

Those models are very exact, because they has been given from cad, with maker's license, in this case the Boeing [8] and The Singapore Airlines, in fact this model has asian company livery.

This model is analyzed through Catia V5r16 software made by Dassault-Systemes [12].

Here are some screenshoot related to data, see figure 3.6



### 3.3 Main geometric parameters

#### 3.3.1 Wing related parameters

Here are some characteristic wing related parameters.

Symbol	Description	Value
$X_{c,le,W}$	Longitudinal distance of wing from the structural reference frame	17.45m
$Z_{c,le,W}$	Height of wing apex from the structural reference frame	−0.75m
$S_W$	Wing planform area	403.36m <sup>2</sup>
$b_W$	Wing span	60.1m
$\Lambda_{le,W}$	Wing sweep angle of leading edge	34.72 deg
$\Lambda_{c/4,W}$	Wing sweep angle of quart of chord	30, 56 deg
$\Gamma_W$	Wing dihedral angle	8.91 deg
$C_{r,W}$	Wing root chord	14.26m
$C_{t,W}$	Wing tip chord	1.76m
$i_W$	Wing incidence (assumed)	2 deg
$\varepsilon_{t,W}$	Wing geometric twist angle (assumed)	0 deg
$(\alpha_{0,l})_{t,W}$	Wing tip airfoil zero lift	−2.2 deg
$(\alpha_{0,l})_{r,W}$	Wing root airfoil zero lift	−1.845 deg
$\lambda$	Taper Ratio	0.123
$\mathcal{R}$	Aspect Ratio	8.955

#### 3.3.2 Horizontal Tail related parameters

Here are some characteristic horizontal tail related parameters.

Symbol	Description	Value
$X_{c,le,H}$	Longitudinal distance of HT from the structural reference frame	48.44m
$Z_{c,le,H}$	Height of HT apex from the structural reference frame	1.62m
$S_H$	HT planform area	84.231m <sup>2</sup>
$b_H$	HT span	20.62m
$\Lambda_{le,H}$	HTail sweep angle of leading edge	40.145 deg
$\Lambda_{c/4,H}$	HTail sweep angle of quarter chord	36.09 deg
$\Gamma_H$	HTail dihedral angle	7.91 deg
$C_{r,H}$	HTail root chord	6.47m
$C_{t,H}$	HTail tip chord	1.7m
$i_H$	HTail incidence (assumed)	−2 deg
$\varepsilon_{t,H}$	HTail geomertic twist (assumed)	0 deg
$(\alpha_{0,l})_{r,H}$	HTail tip airfoil zero lift	−2.865 deg
$\lambda$	Taper Ratio	0, 263

### 3.3.3 Vertical tail related parameters

Here are some characteristic vertical tail parameters.

Symbol	Description	Value
$X_{c,le,H}$	Longitudinal distance of VT from the structural reference frame	44.89m
$Z_{c,le,H}$	Height of VT apex from the structural reference frame	3.20m
$S_H$	VT planform area	$51.64m^2$
$b_H$	VT span	20.62m
$\Lambda_{le,H}$	VT sweep angle of leading edge	45 deg
$\Lambda_{c/4,H}$	VT sweep angle of quarter chord	40.39 deg
$\Gamma_H$	VT dihedral angle	0 deg
$C_{r,H}$	VT root chord	8.19m
$C_{t,H}$	VT tip chord	2.39m
$i_H$	VT incidence	0 deg
$\varepsilon_{t,H}$	VT tip geometric twist angle	0 deg
$(\alpha_{0,l})_{r,H}$	VT airfoil mean zero lift	0 deg

### 3.3.4 Geometric fuselage parameters

Here are some characteristic fuselage parameters

Symbol	Description	Value
$l_b$	Fuselage length	56.7m
$S_{s,B}$	Side area	$301.91m^2$
$w_{max,B}$	Fuselage maximum width	$5.8m^2$
$w_{avg,B}$	Fuselage average width	4.86m
$w_{B,H}$	Fuselage width at horizontal tail	4.60m
$h_{max,B}$	Fuselage maximum height	6.26m
$h_{avg,B}$	Fuselage average height	4.81m
$h_{1/4,B}$	Height at quarter length from the structural reference frame	6.03m
$h_{3/4,B}$	Height at three quarter length from the structural reference frame	5.87m
$h_{B,V}$	Fuselage height at Vertical tail root apex	4.91m

### 3.3.5 Operating points

Symbols	Description	Valore
$V_{AC}$	Flight speed	$296.50607 \frac{m}{s}$
$M_{AC}$	Mach number at specific altitude	0.85
$h_{SL}$	Fight altitude at the sea level	10670m

### 3.4 Longitudinal stability

To have the aircraft longitudinal stability we will refer to matrix coefficients longitudinal stability

$$\begin{bmatrix} C_{D_1} \\ C_{L_1} \\ C_{m_1} \end{bmatrix} = \begin{bmatrix} C_{D_0} & C_{D_\alpha} & 0 & 0 \\ C_{L_0} & C_{L_\alpha} & C_{L_i} & C_{L_{\delta_e}} \\ C_{m_0} & C_{m_\alpha} & C_{m_i} & C_{m_{\delta_e}} \end{bmatrix} \begin{bmatrix} 1 \\ \alpha \\ \delta_e \end{bmatrix} \quad (3.1)$$

In our study cases, considering incidence of horizontal tail  $i$  has known element about the system, the variables become two, so it's possible to consider only the lifting power  $L$  and only pitching moment  $m$ . The number of equations has been become two, so having this system:

$$\begin{bmatrix} C_{L_1} - C_{L_0} - C_{L_i} i w \\ C_{m_1} - C_{m_0} - C_{m_i} i w \end{bmatrix} = \begin{bmatrix} C_{L_\alpha} & C_{L_{\delta_e}} \\ C_{m_\alpha} & C_{m_{\delta_e}} \end{bmatrix} \begin{bmatrix} \alpha \\ \delta_e \end{bmatrix} \quad (3.2)$$

Therefore, to solve it, it needs to detail above coefficients, after placing the condition of axisymmetric balance flight as:

$$C_{L_1} = \frac{2W}{\rho V^2 S_W} = 0,436 \text{ rad}^{-1} \quad (3.3)$$

$$C_{m_1} = 0 \quad (3.4)$$

#### 3.4.1 Lift coefficient dependent on $\alpha$

Following the next formula, we have the lift coefficient deendent on  $\alpha$  from attack angle aircraft that could be represented has:

$$C_{L_\alpha} = C_{L_{\alpha,W}} + C_{L_{\alpha,H}} \eta_H \frac{S_H}{S_W} \left( 1 - \frac{\partial \varepsilon}{\partial \alpha} \right) = 7,975 \text{ rad}^{-1} \quad (3.5)$$

where

$C_{L_{\alpha,W}}$  is the contribution to the lift coefficient dependent on  $\alpha$  given by the wing, in our case according to Polhamus formula:

$$C_{L_\alpha} = \frac{2\pi \mathcal{R}}{2 + \sqrt{\left[ \frac{\mathcal{R}^2(1-M^2)}{k_1^2} \left( 1 + \frac{\tan^2 \Lambda(0.5)}{1-M^2} \right) + 4 \right]}} \quad (3.6)$$

$C_{L_{\alpha,H}}$  is the contribution to the lift coefficient dependent on  $\alpha$  caused by horizontal tail, also calculated in this case according to the Polhamus formula; this coefficient must be reduced by wing area and horizontal tail.

$\eta_H$  is the dynamic pressure coefficient on the horizontal tail;

$\left( 1 - \frac{\partial \varepsilon}{\partial \alpha} \right)$  is the contribution to the downwash effect on the horizontal tail of the aircraft.

### 3.4.2 Determination of aerodynamic center for wing+fuselage

The aerodynamic center is defined to be the point  $\bar{c}$  where pitching moment is independent on the attack angle  $\alpha$ .

To schematize wing+fuselage the aerodynamic center can be calculated as sum of different contributions, whose the first shows the position about aerodynamic center of the wing, and the second the shift caused by fuselage

$$\bar{x}_{AC_{WB}} = \bar{x}_{AC_W} + \Delta x_{AC_B} \quad (3.7)$$

The term  $\bar{x}_{AC_{WB}}$  is drawn from the connection

$$\bar{x}_{AC_{WB}} = K_1 \left( \frac{x'_{AC_B}}{c} - K_2 \right) \quad (3.8)$$

While the term  $\Delta x_{AC_B}$  means the shift of aerodynamic center due to fuselage effect and its calculable according Munk's theory [2] [11] using following relationship:

$$\Delta x_{AC_B} = -\frac{1}{2.92S\bar{c}} \sum_{i=1}^n w_{B_i}^2 \frac{d\bar{\varepsilon}}{d\alpha} \Delta x_i \quad (3.9)$$

Particularly, the term  $\frac{d\bar{\varepsilon}}{d\alpha}$  is calculated with Multhopp method, following the formula we have:

$$x_{AC_{WB}} = 0.488 \quad (3.10)$$

### 3.4.3 Pitching coefficient dependent on $\alpha$

the pitching moment coefficient dependent on  $\alpha$  can be expressed as:

$$C_{M_\alpha} = C_{L_{\alpha, WB}}(\bar{x}_{AC_{WB}} - \bar{x}_{CG}) + C_{L_{\alpha, H}} \eta_H \frac{S_H}{S_W} \left( 1 - \frac{d\varepsilon}{d\alpha} \right) (\bar{x}_{CG} - \bar{x}_{AC_H}) = -3,187 \text{ rad}^{-1} \quad (3.11)$$

We can see the further introduction of the arms pitching moment compared with the centre mass of aircraft; particularly we have:  $(\bar{x}_{AC_{WB}} - \bar{x}_{CG})$  is the arm of lift force application generated by wing area of the boeing than the gravity center about this aircraft; while  $(\bar{x}_{CG} - \bar{x}_{AC_H})$  than we can observe that all distances are no-dimensionals compared with the *middle aerodynamic chord* aircraft.

### 3.4.4 Lift coefficient dependent on $i_h$

The lift coefficient dependent on the incidence angle about horizontal tail can be defined as:

$$C_{L_{i_H}} = \eta_H \frac{S_H}{S} C_{L_\alpha} = 0.92291 \text{ rad}^{-1} \quad (3.12)$$

it can be highlighted that the contribution of tail depending on pitching incidence caused by taking off the lift coefficient of horizontal tail, due to ratio between empennage area and

area named  $S_W$ , il coefficiente di recupero della pressione dinamica  $\eta_H$

### 3.4.5 Pitching coefficient dependent on $i_H$

Similiar to the previos section we have the contribution about horizontal tail dependent on incidence empennage angle:

$$C_{m_{i_H}} = \eta_H \frac{S_H}{S} C_{L_\alpha} (\bar{x}_{AC_H} - \bar{x}_{CG}) = -2,975 \text{ rad}^{-1} \quad (3.13)$$

We have just explained those terms before.

### 3.4.6 Elevator's moment

The deflection effect of elevator on longitudinal stability is showed by two coefficient  $C_{m_{\delta_e}}$  and  $C_{L_{\delta_e}}$ . With regard to the contribution given to lift coefficient aircraft dependent on deflection elevators on vertical tail, the  $C_{L_{\delta_e}}$  is:

$$C_{L_{\delta_e}} = C_{L_{i_H}} \tau_e = \eta_H \frac{S_H}{S} C_{L_{\alpha, H}} \tau_e = 0,415 \text{ rad}^{-1} \quad (3.14)$$

while the contribution to the lift moment can be explained as:

$$C_{m_{\delta_e}} = \eta_H \frac{S_H}{S} C_{L_{\alpha, H}} (\bar{x}_{CG} - \bar{x}_{AC_H}) = -1,339 \text{ rad}^{-1} \quad (3.15)$$

Also in this case there is simmetry in formulas (vedi riferimento altra formula)

### 3.4.7 Stability analysis

Well-known all coefficients, the system in our case become:

$$\begin{bmatrix} C_{L_1} - C_{L_{i_H}} i_H - C_{L_0} \\ C_{m_1} - C_{m_{i_H}} i_H - C_{m_0} \end{bmatrix} = \begin{bmatrix} C_{L_\alpha} & C_{L_{\delta_e}} \\ C_{m_\alpha} & C_{m_{\delta_e}} \end{bmatrix} \begin{bmatrix} \alpha \\ \delta_e \end{bmatrix} \quad (3.16)$$

After solving this system with MArYSA we have the attack angle value of the aircraft and the deflection angles of elevator that allow a symmetric and balance longitudinal flight.

$$\alpha_e = -0.865 \quad (3.17)$$

$$\delta_e = -0.028 \quad (3.18)$$



---

# BIBLIOGRAPHY

---

- [1] M. Napolitano (2012), *Aircrafts Dynamics: From Modeling to Simulation*, John Wiley & Sons Inc.
- [2] D. E. Hoak (1960), *The USAF Stability and Control DATCOM*, Air Force Wright Aeronautical Laboratories
- [3] *Esdu* su *esdu* 2014. <http://www.esdu.com/cgi-bin/>
- [4] *Mathcad* su PTC 2014. <http://it.ptc.com/product/mathcad/>
- [5] *Hierical Data Format* su HDF group 2014. <http://www.hdfgroup.org/HDF5/>
- [6] B. N. Pamadi (1998), *Performace, Stability, Dynamics and Control of Airplanes*, American Institute of Aeronautics and Astronautics Inc.
- [7] L. Pantieri, T. Gordoni (2008-2012), *L'arte di scrivere con  $\text{\LaTeX}$* ,
- [8] *787 Dreamliner* su Boeing 2014. <http://grabcad.com/library/boeing-787-dreamliner>
- [9] *787 Dreamliner* su Wikipedia 2014. [http://it.wikipedia.org/wiki/Boeing\\_787\\_Dreamliner](http://it.wikipedia.org/wiki/Boeing_787_Dreamliner)
- [10] *787 Dreamliner* su Grabcad 2014. <http://grabcad.com/library/boeing-787-dreamliner>
- [11] Roskam, J. *Airplane Flight Dynamics and Automatic Flight Controls-Part I. Design, Analysis and Research Corporation*, Lawrence, KS, 1995
- [12] *Catia V5* su 3ds 2014. <http://www.3ds.com/it/prodotti-e-servizi/catia/>